# THEORETICAL PREDICTION OF MECHANICAL BEHAVIOR OF REGULAR AND CHIRAL HONEYCOMBS BASED ON LOADING OF SINGLE CELL.

**BY**

**SAI KRISHNA PINNAMANENI**

Presented to the Faculty of the Graduate School of

The University of Texas at Arlington in Partial Fulfillment

Of the Requirements for the Degree of

**DOCTOR OF PHILOSOPHY IN MECHANICAL ENGINEERING**

**THE UNIVERSITY OF TEXAS AT ARLINGTON**

**DECEMBER 2021**

SUPERVISING COMMITTEE:

Dr. Andrey Beyle, Advisor

Dr. Dereje Agonafer, Chair

Dr. Kent Lawrence, Co-Advisor

Dr. Miguel Amaya

Dr. Rajesh Kasukurthy

Acknowledgments

I would like to express my appreciation and very thank my thesis advisor Dr. Andrey Beyle, for the opportunity to work on interesting projects and continued support since the beginning of my first day. Dr. Beyle has always been very supportive, guidance and mentorship throughout my dissertation. I would also extend my gratitude to Dr. Dereje Agonafer for his endless support, unconditional availability throughout my work. I'm very grateful to Dr. Agonafer for accepting to act as committee chair and for his time during the course.

I would also extend my appreciation for Dr. Kent Lawrence for his valuable suggestions and encouragement. I was always pleasured to work with Dr. Lawrence during my teaching assistant and enjoyed working with him every semester. I also like to thank Dr. Amaya for his valuable time and suggestions on my research and feel very grateful for his ideas and for providing resources.

I also like to extend my gratitude to Dr. Rajesh Kasukurthy for his valuable suggestions and for being very supportive throughout my entire Ph.D., Ph.D. Rajesh Kasukurthy was providing me with all things needed for my research and was always available to speak and provide me suggestions.

Finally, I would like to thank my parents Venkateshwara Rao Pinnamaneni, Sunitha Pinnamaneni for their continuous support throughout my journey and for giving me every emotional and financial help. I would also extend my gratitude and thanks to my brother Sri Chaitanya Pinnamaneni for his continuous support and for providing me with valuable suggestions throughout my Ph.D.

I will take this moment to also appreciate and be very grateful to my cousin brother Partha Pudhota and Dr. Sunitha Pudhota who were very encouraging and supportive during my dissertation and research.

Dedicated to my parents, brother, and friends.

Abstract

Cellular solids are both naturally occurring and man-made materials depending on the characteristic length or Stochastic manner, these materials exhibit a low-relative density usually 30% than the constituent solid material. Low-density cellular solids have been demonstrating superior mechanical properties in various applications from marine to aerospace and lightweight sandwich structures, which has intrigued in development of novel structured materials.

Cellular solids offer great design flexibility ashowows how for the targeted geometric for the application-based industry. These materials are used in sandwich structures and come in the shape of hexagonal. An additional aspect of determining the properties and behavior is by studying single cells which can be incorporated into the sandwich panel. It has been difficult to determine the exact shape or geometry to be used based on the application, we investigate the chiral and standard hexagonal honeycomb to design the novel macrostructural and the topology of the chiral shapes to control both the static and dynamic behavior phenomena.

This particular cellular structure exploits the high stiffness of the honeycomb core and also absorbs energy on impact. The present research being addressed shows the comparison and the suitable geometry based on the application.

Table of Contents

LIST OF FIGURES

# Chapter 1

## INTRODUCTION

Composite materials are widely used in today's modern world in commercial as well as in various applications and are also considered engineering marvels because of the properties they exhibit. The composite materials usually come in sandwich structures which are in the form of sandwich structure where the laminate and lamina are in the form of skin outer part of the core adhesive with the core. Cellular honeycombs are very unique in exhibiting as energy-absorbing components which are used in aircraft, marine, and various high energy absorption-based applications. A major challenge in this field is to understand the properties of the honeycomb structures in design optimization and their performance in Mechanical, Thermal and acoustic.

Honeycomb structures with hexagonal shapes are the most commonly used cellular materials and because of their vast demand in Engineering applications they have been manufactured with various technologies based on application, however in reality based on rapidly increasing diversity in micro and macro scale point of view, the shapes of different cell have been evolved, for example, honeycomb structure comes in hexagonal, rectangular, and triangular shape and recently with the chiral shapes showing more advantage and exhibiting better properties brings attention to develop and improve the characteristics of the cell geometry.

Cellular materials like honeycomb sandwich structures come with three components, which is skin with top and bottom and core is in between sandwich. These sandwich panels are used where high bending stiffness is required with minimum weight, they also exhibit high strength to weight ratio and low weight for a given stiffness can be increased by the only the thickness of the core is increased.

Honeycomb structures as said come in three components, skin or face sheets are made up of materials with high strength such as a metal plate or fiber-reinforced polymer composite, the design of the face sheet is so important because it is the main component for load-carrying capacity with high specific bending stiffness, when combined with high specific strength it results in low weight and highly efficient component, the honeycomb structures are used since 3000 years ago in various structures which are inspired from nature.


Fig 1.1 Pantheon of Rome interior Structure.

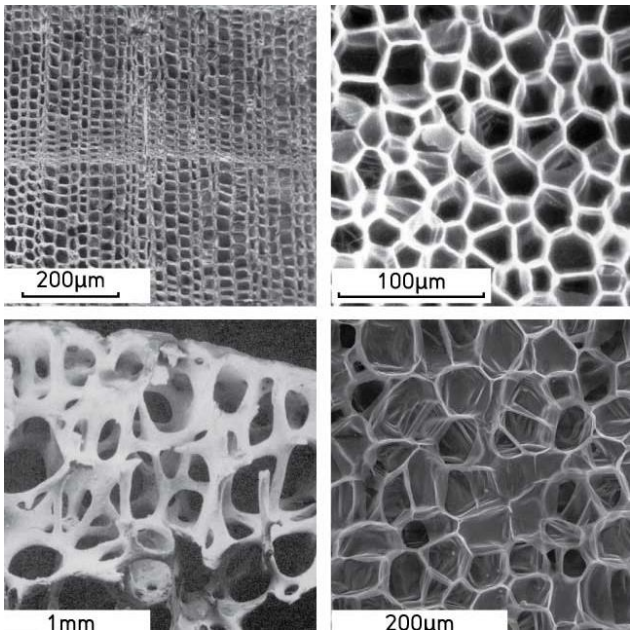


Figure 1.2 Trabecular bone and parenchyma structure at the microscopic level

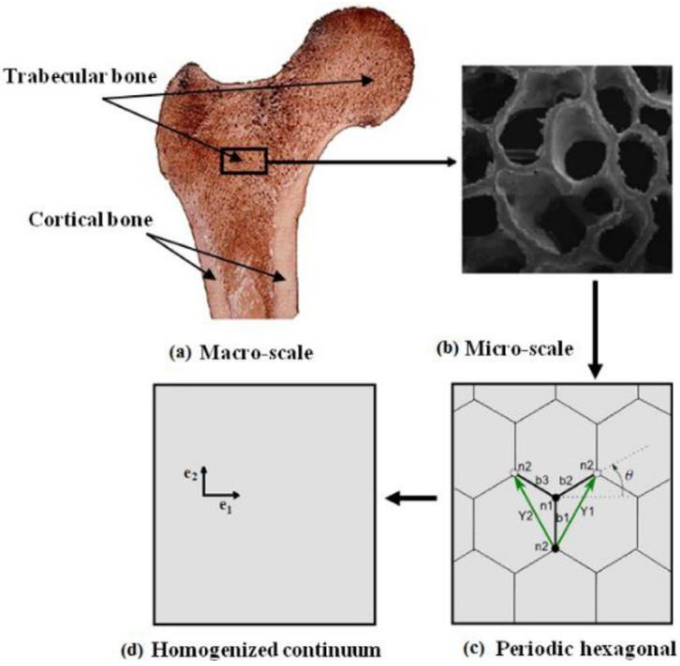


Figure 1.3 Microstructure and homogenization of the bone compared with honeycomb.

Honeycomb structure panels are low modulus and lightweight cellular core, the assembly maximizes stiffness-to-weight ratio and bending strength-to-weight ratio, which effectively helps to carry distributed load across the panel, one of the main components is core which has the role of bearing out-of-plane shear stress.

The Honeycombs, with prismatic cells, are also called two-dimensional cellular solids and the relative density is the ratio of the density of the cellular solid made from to the equivalent to the volume fraction of the solid. If the structure has foam and is in polyhedral shape is called three-dimensional cellular solids.

### 1.1 Motivation and Methodology

Cellular solids have a very peculiar property that attracts and is inspired by nature, the investigation and development of cellular solids as an energy-absorbing component to various spacecraft fuselage designs has always been kept an open mind of looking out of other patterns or designs that ever existed in Honeycomb structures.
Honeycomb structures are already been used in the fuselage of aircraft, building spacecraft, and also in automotive, marine applications, previous studies have been conducted in regular hexagonal shape but not on different topologies which can help understanding better geometries and their properties in a real-world application, Cellular solids are found in nature predominately for example skull of birds and humans the outermost layer is nothing but the sandwich structure which help us protect from any impact from outside.

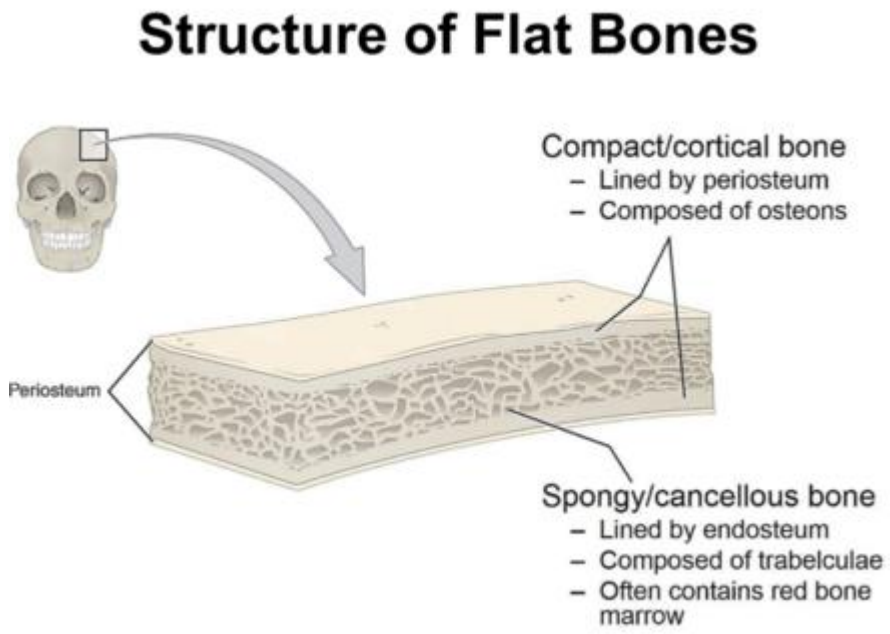


Figure 1.4 Structure of Flat bone

The motivation of this study is to investigate various shapes along with chiral figures and compare the results for the optimal design for various applications, the core is the main part of the structure and involves more with the bending stiffness. The skins are responsible for the load-bearing and transmitting the load to the core, usually, the skin materials are made up of epoxy-resin, thermoplastic, aluminum, and Nomex, and the core is made up of usually fiberglass, carbon fiber, and reinforced plastic and they vary based on their application from jet aircraft to wind turbine blades.

## 1.2 Thesis Outline

Chapter 2 consists of a literature review and also a discussion with an introduction to the topology of hexagonal honeycomb and various chiral shapes, we use SOLIDWORKS and ANSYS for the simulation and computational evaluation. Hexagonal shapes honeycomb with a single-cell and with the panel is being studied and the geometry modeling is carried out in SOLIDWORKS and then the file is being imported to ANSYS and the simulation is given a run and the results are obtained.

The computational method is discussed in Chapter 3 or Methodology and the 3 Dimensional models are created and mesh convergence study has also been conducted to validate the results obtained, in this dissertation mainly two objectives of study has been conducted one is a hexagonal single cell and a sandwich panel has been modeled and simulations are carried out and the second part is the 4 different chiral shapes are modeled and ANSYS simulation is performed with both impact of sandwich panels and other single-cell components.

Chapter 4 includes the results and discussion of the models and comparison of the simulations are been conducted by varying the thickness of the face sheet and also the chiral shapes are so independent to each other in terms of their appearances, and the

results show the effects behind the structural behavior under various loading and the deformation of the cells a stress-strain study is also been conducted.

Chapter 5 includes the discussion of the results and discussion from the comparison of the various geometries and modeled in various tools like SOLIDWORKS AND ANSYS and chapter 6 includes conclusion and future work of the research and finally with the references.

# Chapter 2

## Literature Review

Any metal when loaded with weight or in bending mode it causes huge stress and strain, the deformation depends on various factors like the type of material, the thickness of the metal, and type of the environmental conditions and the manufacturing process includes a lot of defects and pores which can be avoided but cannot completely be terminated. Coming to the composite materials made up of different materials they exhibit unique features and perform better than traditional metal components. Cellular materials include a honeycomb structure in which the three components, the bottom, and top are called skin or face sheets, and the center in between them are called core.

Chiral honeycombs of elastic constants of 3-,4- and 6- connected chiral honeycombs which are subjected by uniaxial in-plane loading have been studied by [] and tetrarchical honeycombs have been carried out using the Abaqus software with 8 node quadratic elements. The deformation of the ligament mid-points of the chiral honeycombs remains parallel to the honeycombs. They found that in-plane young's moduli and Poisson's ratio of hexachiral, tetrachiral, anti-tetrachiral, trichiral, and anti-archival are all found to be in a good argument with FE Model predictions. It was found that the young's modulus has been increasing with ligament coordination number. The auxetic honeycombs have the value of Poisson's ratio close to -1. The trichiral has the positive Poisson's ratio whereas the anti-trichiral shows a negative Poisson's ratio.

The study of elastic buckling of chiral hexagonal cells has been studied by [] and the work is carried out to study both analytical, numerical, and experimental on the compressive strength of hexagonal chiral honeycombs. These cells are considered under noncentrosymmetric single cell with negative Poisson's ratio with the value of -1.

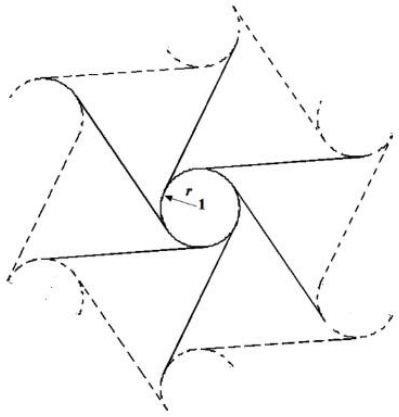


Figure Unit cell of the chiral honeycomb.

The compressive strength of the auxetic hexagonal chiral honeycombs has been modeled using both analytical and Finite element approach, the study shows that cylinders are considered the providers of the majority of the compressive strength and the FE Simulations has shown that nodes behave like cylindrical shells under axial uniform loading that has some deformations in the localized. The Hexagonal chiral shapes are have been showing consistently potentially used in the sandwich light materials. The compressive strength for low-density ratios appears to be higher compared to analogous density properties in conventional centrosymmetric honeycombs. The more complex nodes under buckling interaction between nodes and the plates of the cells are studied are requiring some attention to design new cellular structures.

The prediction of effective elastic modulo of honeycomb-type sandwich plates has been studied by []. The sandwich panels consist of a honeycomb core with regular hexagonal cells and the orthogonal fiber-reinforced face sheets where the considerations on the cellular structure have been investigated and the results showed are out-of-plane shear properties of the core ($G_{xy}$, $G_{yz}$) may be calculated by different models.

Vinson, Zhang and Ashby, and Kobe Levi have given equations for the compressive young's modulus.

The investigations of compressed sandwich composite/honeycomb cylindrical shell are subjected to compressive loads and o detect the initiation of overall buckling mode the strain gauges are applied and was studied by []. The failure analysis of deep and curved or thick cylindrical panels is made of a cellular honeycomb. The first failure mode was identified as the overall buckling and the mode by 8.5% higher than experimental results is not high and acceptable. The second mode of failure was the face sheet wrinkling because of the manufacturing imperfections of the core and the interface between the skin and core.

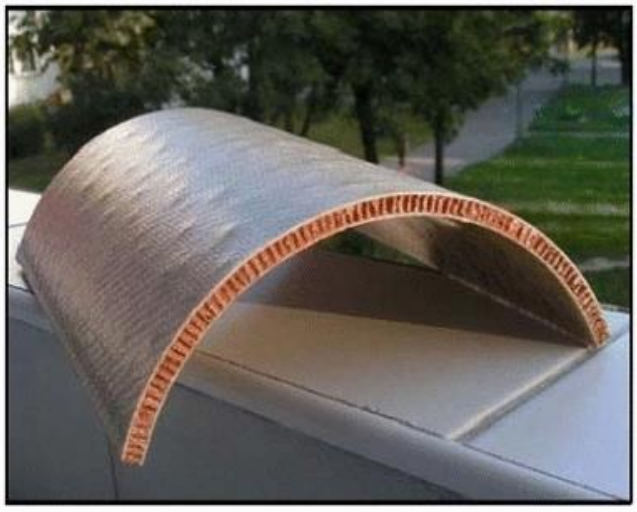

The properties of chiral honeycombs are discussed by [] the unusual cellular solids created new interest in re-entrant structure this unique honeycomb structure exhibits negative Poisson's ratio, all the allowable ranges is closer to 0.33. 2-D honeycomb with regular regular hexagonal cells has Poisson's ratio of +1 and the out-of-plane properties differ due too anisotropic. Foam materials with a negative Poisson's ratio can go up to -0.7 an inverted or re-entrant cell structure is obtained from isotropic permanent volumetric compression form.

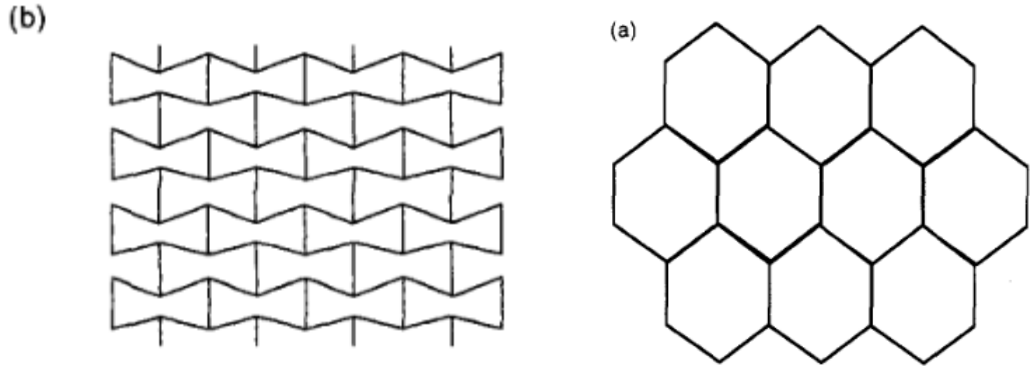


Figure 2.2 Regular vs re-entrant hexagonal honeycombs.

The transverse elastic properties of 5 different chiral honeycomb shapes are discussed by []

Auxetic behavior in honeycombs can be achieved with specific cell geometries, including center-symmetric re-entrant bow-shaped cells and the out-of-plane linear elastic properties of hexachiral, tetrachiral honeycombs have been investigated using analytical and finite element methods, from the theoretical point of view the transverse shear modulus is bounded between upper and lower bound. The compressive modulus is calculated from cellular solids.

$$\frac{E_z}{E_{core}} = \frac{\rho}{\rho_{core}}$$

$E_{core}$ and $\rho_{core}$ are the modulus and density of the solid material.

$$\frac{\rho}{\rho_{core}} = \frac{\beta[3\alpha + \pi(2-\beta) - 3[\varphi - (1-\beta)sin\varphi]}{2\sqrt{3}[\left(1-\frac{\beta}{2}\right)^2 + \frac{\alpha^2}{4}]}$$

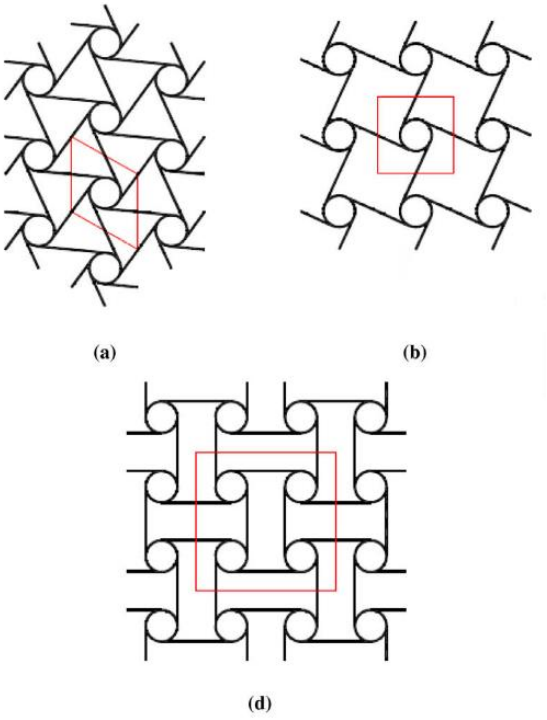


Figure 2.3 Different types of Chiral honeycomb structures.

Regular and chiral shape honeycombs material properties are described by Gibson Ashby in Cellular solids, foams can be made out of metals, plastics, ceramics, and even glasses. The geometric structure of the foam decides the size and shape of the cells.

The cell wall properties which are usually $\rho_s$ density, young's modulus $E_s$, the plastic yield strength $\sigma_{ys}$, fracture strength $\sigma_{fs}$, the thermal conductivity $\lambda_s$ and thermal expansion $\alpha_s$, these properties help us understand more on how the cellular materials behave and their applications

are fitted, they are used in a wide variety of applications and the best common are polymer and metal ones of the core of sandwich panels from making furniture to aerospace applications. Metal-based honeycombs are mainly used in aerospace engineering and energy-absorbing applications and ceramic-based honeycombs are used in high-temperature applications and many natural materials like wood and bamboos are used in structures and load-bearing applications.

The cell walls have a very intricate 3-Dimensional network that distorts during deformation and it's very difficult to identify. If a honeycomb is compressed in-plane the cell walls first bend by giving linear elastic deformation and the cell collapse by elastic buckling, plastic yielding and yield creep, or even by brittle fracture which completely depends on cell wall material. Usually, the cell wall stops collapsing when the adjacent cell walls touch each other and the structure densifies by increasing stiffness rapidly. The tension in the cell walls first bends but the elastic buckling is not possible and the cell wall material yields plastically. If the cell walls are brittle it fractures. The large scale honeycomb structure model are made up of rubber, metal, or ceramic. If the cell walls are under out-of-plane deformation the stress acts parallel to the axis of the prismatic cells and the cell walls suffer extension or compression and the moduli make the collapse stress are much higher.

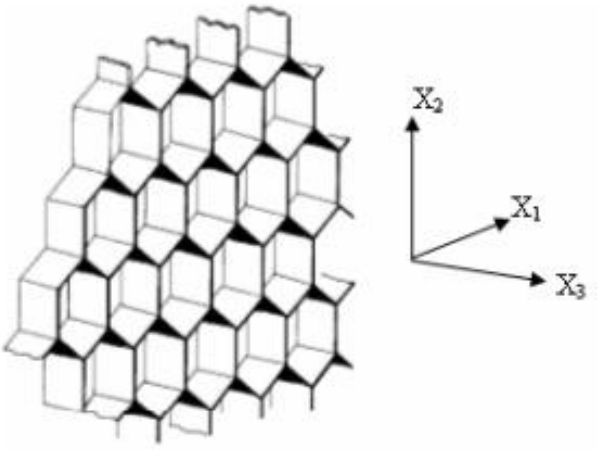

Figure 2.4 Honeycomb loading directions.

The in-plane loading is in the $X_1$ and $X_2$ direction and the out-of-plane is $X_3$ direction, the in-plane stiffness and strengths are the lowest because the stresses in this plane make the cell walls bend. The out-of-plane stiffness and strength are much larger because they require the axial extension or compression of the walls. The study of in-plane properties helps us understand more mechanisms by which the cellular solids deform and fail, the out-of-plane analysis gives the additional information on stiffness that is needed to design the honeycomb structure and the behavior of the natural honeycombs like materials include wood and polymers.

The compressive and tensile stress-strain curves for elastomeric and elastic-plastic honeycomb and one which is elastic-brittle. In compression linear-elastic regime by a plateau of approximation constant stress which leads into a final regime of steeply increasing stress and each regime with the mechanism of deformation which can be identified by loading of honeycombs. The out-of-plane loading is applied mostly in the energy absorption applications where the load and the stress caused due to it is transmitted to the core and the cell wall starts buckling after the threshold limit.

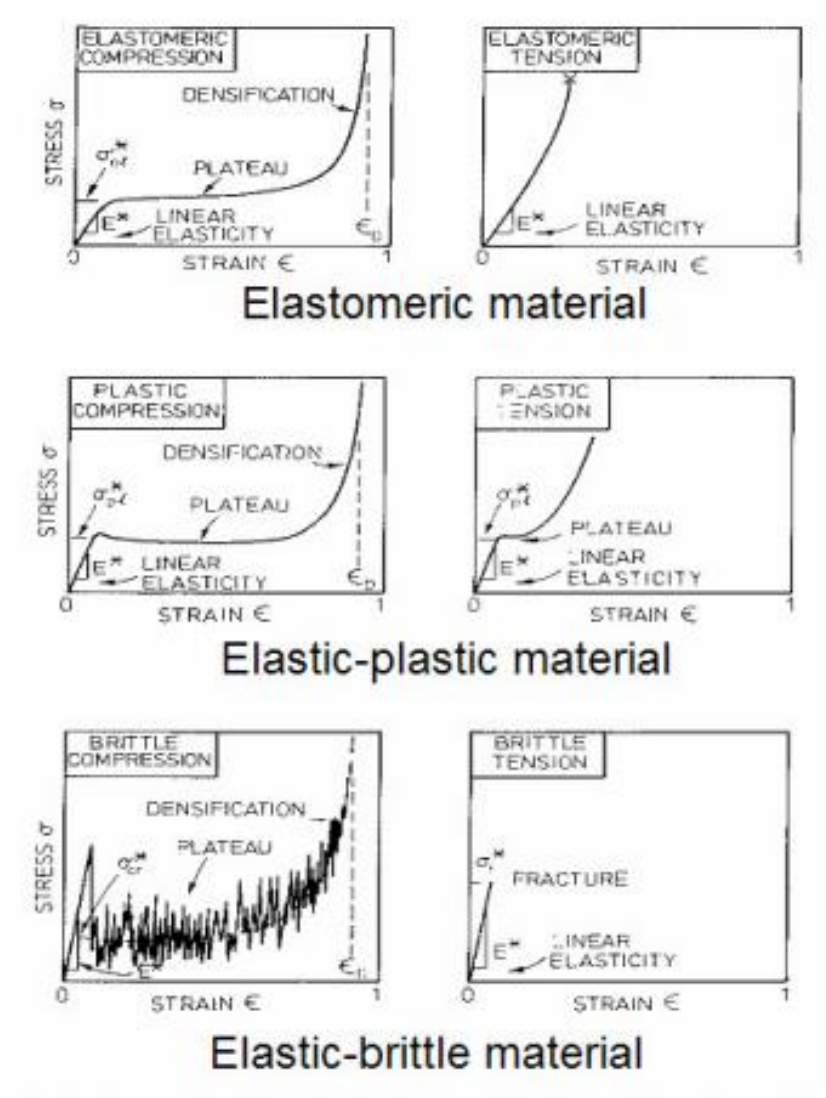


Figure 2.6 Compressive and tensile curves for honeycomb

The first loading causes the cell walls to bend and give the linear elasticity, but when the critical stress is once reached the cell walls being to collapse, and in elastomeric materials collapse to the point where the plastic hinges at the section of the maximum moment in the bent members and brittle materials or by the brittle fracture of the cell walls and eventually high strains the cell collapse sufficiently which opposes cell walls touching the further deformation compresses the cell wall material, stress-strain curve is labeled as densification.

The increase in the relative density of the honeycomb increases the relative thickness of the walls. The resistance to cell wall bending with cell collapse caused higher modulus and plateau stress and the cell walls come close to each other which triggers the densification and the stress-strain curve changes with increasing relative density t/l.

We should also discuss on Voronoi honeycomb which is explained by Ashby Gibson []. These foams are sometimes made up of supersaturating liquid with gas and then reducing the pressure, so the bubble nucleate grows. Voronoi honeycomb is the type of structure which represents the result of nucleation of growth from bubbles, they are created by forming the perpendicular bisectors between random nucleation points and the envelope of surfaces that surround each other. Each cell contains all points that are closer to its nucleation point than any other structure.

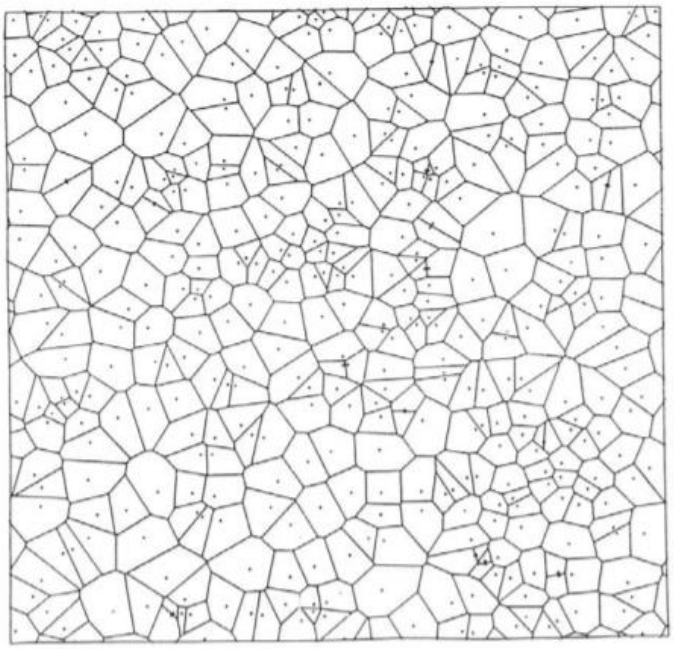

Fig 2.5 Voronoi structured honeycomb

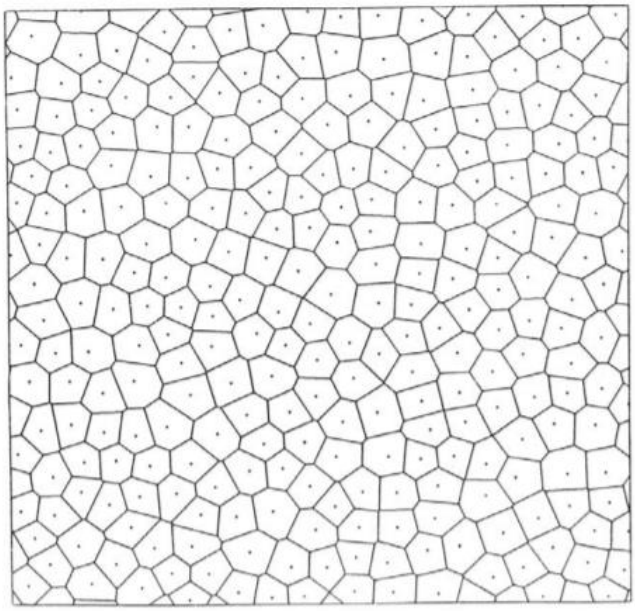

Figure 2.6 Voronoi Honeycomb with exclusive distance.

If all the cells nucleate and grow simultaneously in space at a single isotropic rate. To model the structure of irregular honeycomb we need n points which are firstly generated in a central square with area $a_0$ and periodic boundary conditions. Each cell is constructed by the perpendicular bisectors of the lines connecting this seed to every seed may be obtained by constructing, when the honeycomb model is placed under strain and the periodic boundary conditions corresponding nodes on the opposite edges of the unit cell have identical orientations.

The size of the unit honeycomb cell is given by the stresses reduced by $\rho^3$ and the young's modulus $E_s$ and it's give as

$$\bar{\sigma} = \frac{\sigma}{E_s.\rho 3}$$

The solid material is assumed to be elastic throughout the deformation and the adoption of reduced stress.

Sandwich panel components and constructions have been discussed earlier, where the core is made up of usually Nomex honeycomb and made of metal or foam with open or closed cells. Usually, Nomex is made up of nylon or sometimes aramid which is also from a piece of paper. Several sheets of Nomex paper have glued each other over sequential as multiple layers. They have high density; help prevent moisture penetration open cell-to-cell engagement and have stiffer mechanical properties. Many times, certain manufacturing defects like wrinkling can cause the structure to fail and collapse.

When a simply supported sandwich panel is subjected to in-plane compressive loads, buckling failure can occur. Buckling is characterized by a sudden out-of-plane deformation of the sandwich panel. Buckling of honeycomb structure occurs when the load is applied out-of-plane and there is a deformation that can lead to buckling but happens only when the height of the sandwich structure is greater than the length of the overall sandwich structure.

Buckling of the sandwich structure occurs in several ways and one mode the face sheet layers, and the core has the same amount of experience for the same out-of-plane deformation, which is called global buckling mode, as the deformation is like a long wavelength that is equal to the length of the flat sandwich plate. Another buckling mode is a short wavelength and the face sheet or the core layer they don't extend laterally to the thickness of the immediate layer. This mode is usually called asymmetric buckling mode and the short wavelength mode is the core material is stretched or compressed is called asymmetric buckling mode.

The overall deformation of the sandwich panel can be calculated and studied for the determination of the critical buckling load and different buckling modes of failure which response is core stiffness and core shear strength and as well panel surface dimensions or thickness.

Usually, the honeycomb structure fails by the failure of face, transverse shear failure, Crush of the core, general buckling, shear crimpling, and wrinkling of the face. This failure depends on the loading direction of the component.

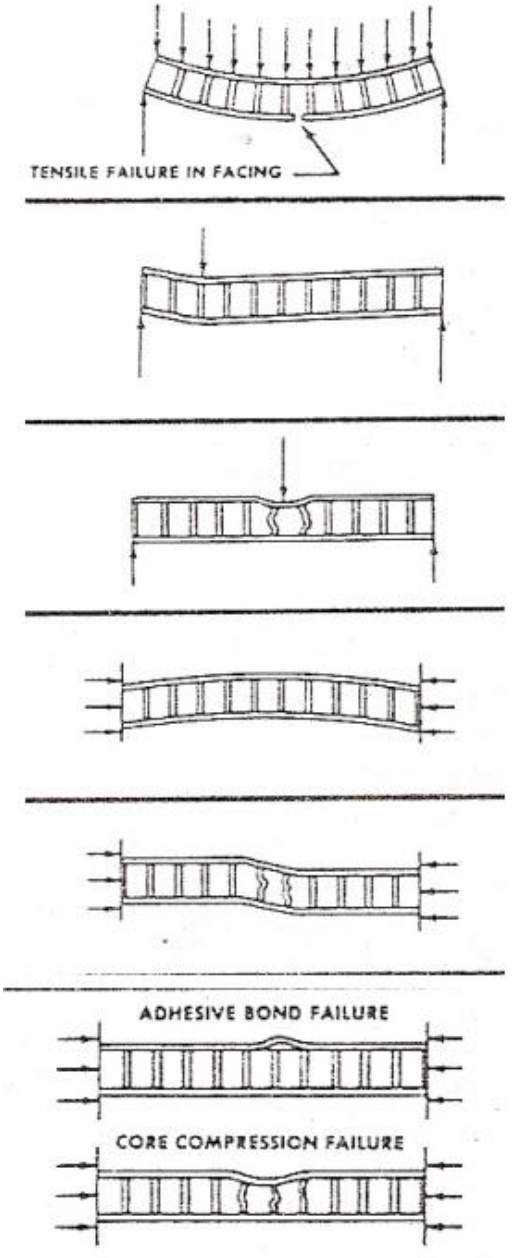


Figure 2.7 Different failure stages of sandwich panel.

The honeycomb structure can be compared with the regular hexagonal panel and numerous studies show the relative stiffness, strength, and weight exceptional. Ashby Gibson has studied various properties of the honeycomb sandwich panels and they have more advantages than conventional metal because of extreme relative stiffness, relative weight.

In the study when we apply out-of-plane de rmation loading on cell length with varying thickness and the cell walls of honeycomb initially compress and the axially so that the young's modulus with volume fraction or the relative density which is $\rho_*$ = density of honeycomb, $\rho_s$ = density of the solid.

$$\text{Relative density} = \frac{\rho_*}{\rho_s}$$

Finite element analysis of the dynamic response of honeycomb structure of low-velocity impact is been studied by []. FEA has been performed in different software on impact velocities of the honeycomb structure and the three main components which include the skin, core, and the bullet, with the same thickness on the strain, stress, and displacement of structure and the sudden collapse of the impact energy.

Cells that come in different shapes and sizes in which the 2D arrays with regular shapes or assemblies of triangles, squares, and hexagonal, but in nature, they are various frequent change or deviations from regular cells caused from the rearrangements. The Voronoi honeycomb for example in the size of dispersion based on size and the varying in the number of edges per cell.

Chiral honeycomb with buckling behavior is studied by []. In this study, an analytical formula and the finite element method are been compared based on the applied boundary conditions. This different chiral geometry has been very intrigued by their behavior and results compared to the conventional honeycomb structure.

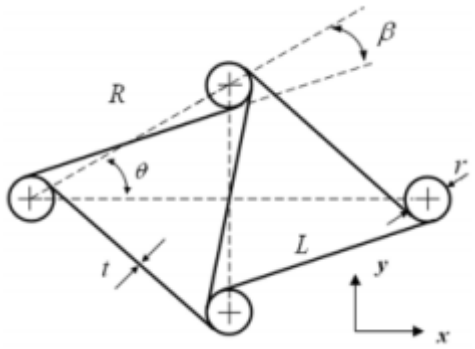


Figure 2.8 Chiral shape of the honeycomb structure

$$\text{Sin } \beta = \frac{2r}{R} \text{ and } \tan \beta = \frac{2r}{L}$$

The distance between the center of adjacent nodes is R and while L, r are the length and the radius of the nodes and the angle β is the orientation of the length to the center of the nodes.

The $P_{cr}$ is the critical load

$$P_{cr} = \frac{KE_s}{\left(1-\upsilon_s^2\right)}\frac{t^3}{L}$$

The critical buckling stress is given by

$$\sigma_{cr} = \frac{E_s}{\sqrt{3\left(1-\upsilon_s^2\right)}}\frac{t}{r}$$

Chapter 3

# METHODOLOGY

There are multiple reasons why we consider honeycomb structures more superior than conventional metals, honeycomb bee has regular prismatic hexagonal cells of cellular solids in two dimensions. The shapes come in different geometries from triangular, square, or rhombus. They are widely used in polymer and metal ones for the core of sandwich panels in everything.

An increase in relative density can be different and the cell walls bend, giving linear-elastic deformation with the same slope as in compression, in case of tension elastomeric honeycomb doesn't buckle but instead cell walls rotate towards the tensile axis, and which causes stiffness to increase. On the other hand, the plastic honeycomb behaves in almost the same way as they do in compression and the plastic hinges form allowing large deformations at a "plateau" stress and the only geometry change which causes nudging the tensile curve above the compression one. Brittle honeycomb fails abruptly in tension and stress which is lower than the crushing strength. In the brittle solid, fracture in tension is controlled by the largest crack or damaged cell, increasing in relative density has a similar effect to that in compression, and the elastic moduli, plastic yield stress, and brittle fracture stress all increase.

In this dissertation we will use different geometries to study on the behavior of honeycomb structures subjected to loading and boundary conditions, we use ANSYS, Solidworks to perform analysis and the results are compared. The mesh independent study I have been conducted to check the mesh quality and validate the analysis.

In this study we first start with the Single-cell honeycomb with varying cell dimensions of 3mm,5mm, and 10mm and the mesh study has been conducted for the mesh size of 0.1mm for the analysis. For the mesh independence study, the mesh sizes used are varying from 0.05,0.075,0.1 and 0.125mm and the elements, nodes are tabulated, and the comparison is being conducted which 0.1mm best suited the analysis.

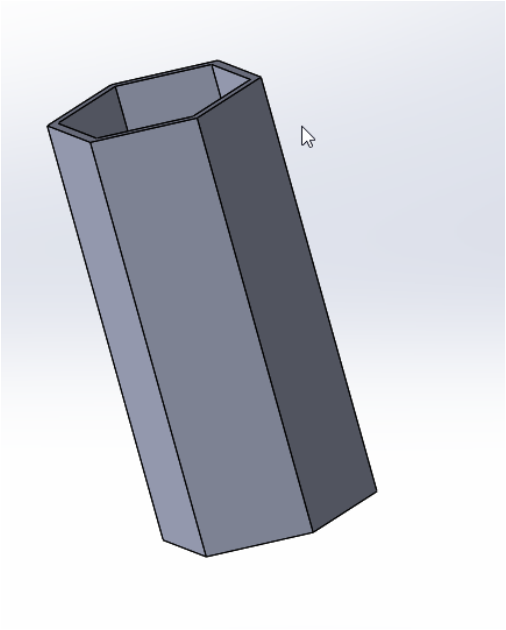

Figure 2.9 Single-cell Honeycomb Geometry using Solidworks

The cell geometry has a cell height of 20 mm and the thickness of the cell is 0.5 mm and the cell length is 3mm which is fixed and the study was conducted for the varying cell sizes from 3,5 and 10 mm and the height, thickness are fixed and not changed for the rest of the simulation.

Mesh was created for various geometries and with varying cell lengths and the results are tabulated. The Mesh sizes used for this study are ranging from 0.05mm, 0.075mm,0.1mm, 0.125mm, and the nodes and elements are calculated for each mesh size.

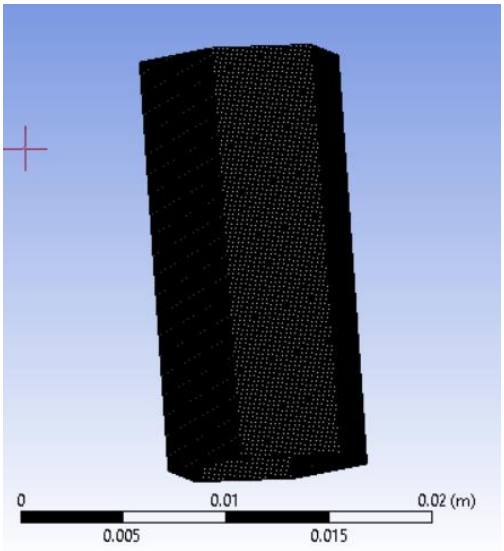


Fig 2.10 Mesh of the geometry

The results obtained from mesh independent study (0.1mm) were chosen to run the further simulation and the nodes and element converged to the adjacent mesh size.

| Mesh Size (mm) | Elements | Nodes | Von-Mises Stress (MPA) | CPU Time |
|---|---|---|---|---|
| 0.05 | 2092400 | 9063211 | 161 | 42m 14sec |
| 0.075 | 614901 | 2773259 | 144 | 28m 24sec |
| 0.1 | 261600 | 1221292 | 134 | 17m 37sec |
| 0.125 | 135680 | 655564 | 126 | 11m 47sec |
| 0.15 | 77318 | 388571 | 118 | 7m 15sec |

Fig 2.11 Tabulated mesh size with elements and nodes

We have concluded based on the elements, nodes and von-mises stress the mesh size of 0.1mm looks very reasonable and optimizing to obtain simulations without any manipulations or results being undesirable, in the mesh study we used quadrilateral elements and a fine mesh was applied.

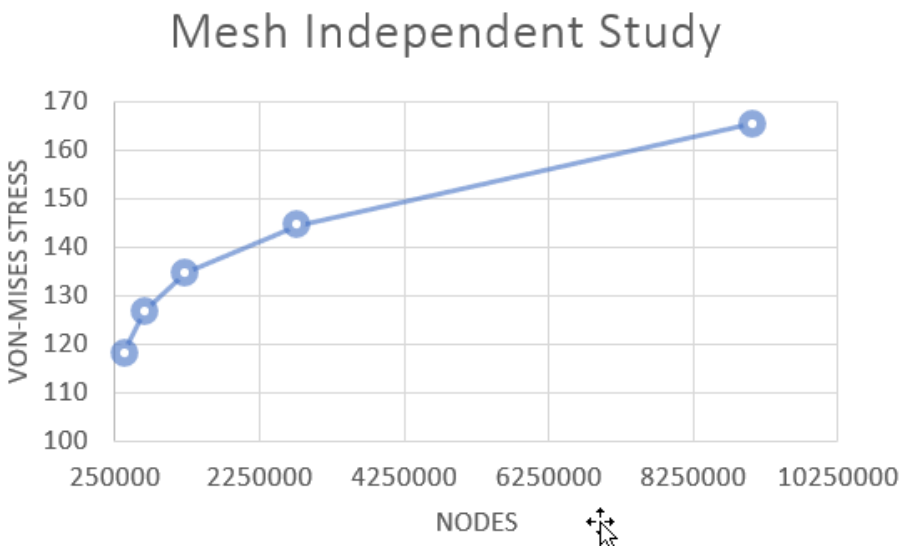


Fig 2.12 Von-Misses stress vs nodes

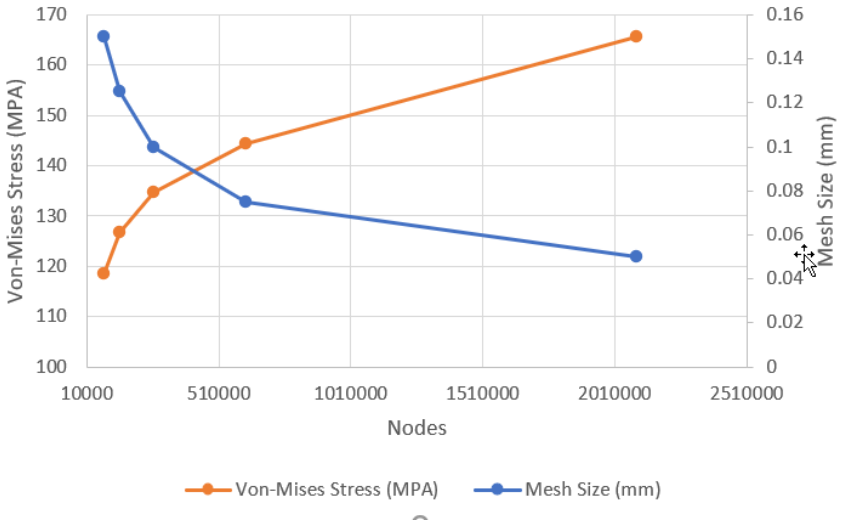


Fig 2.13 Von-Misses stress vs mesh size

Table 2.11 shows that an increase in mesh size can cause a decrease in elements and nodes, the von-misses stress also keeps decreasing significantly. The optimum mesh size and which can validate the results mesh size is used. In the Mesh independent study von-misses stress is plotted along with the mesh size and nodes.

The Von-Misses stress keeps increasing and the graph shows there is an exponential increment in the von-mises stress with an increase in mesh size, the stress has a very low difference and eventually after 0.125mm mesh size the percentage of error has steep high since the von-misses stress is considered as one of the important factors to determine the strength and the stiffness of the materials based on the loading conditions. We tried to apply the same mesh independent study and sizes for the other geometries including the various figures and chiral shapes.

We conduct the mesh independence study for various sizes it helps us to understand more about the geometry and also identify the elements which are sensitive and cause failure. If the model is small and the number of the elements can be increased and simulation is performed to study the behavior under loading conditions. The Mesh independence study also validates the accuracy of the simulations and validates the results. Using appropriate mesh sizes and methods could help us understand the dynamics of the component.

In the out-of-plane behavior of honeycomb structure, we use the 3D-Modeled in Solidworks and then the simulations are generated in the ANSYS workbench, we carry out the mesh sizes and comparison is made between elements and nodes for the von-mises stress and equivalent deformation.

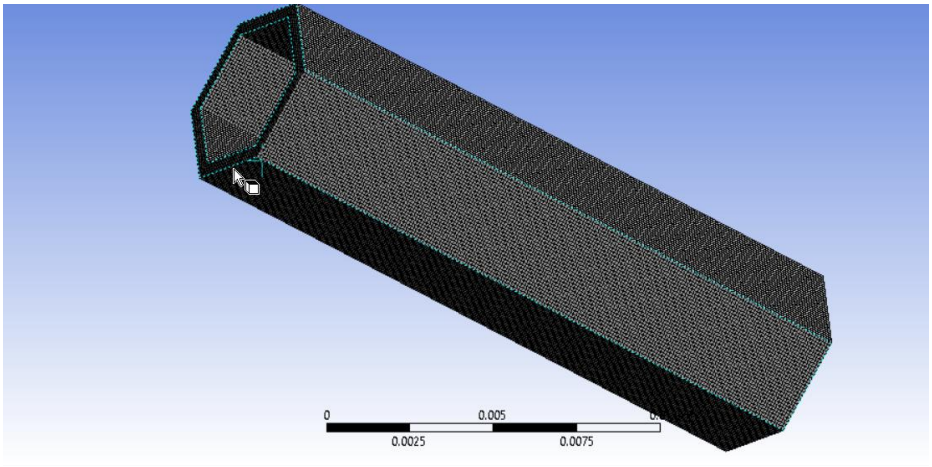


Fig 2.14 Mesh elements for the single cell

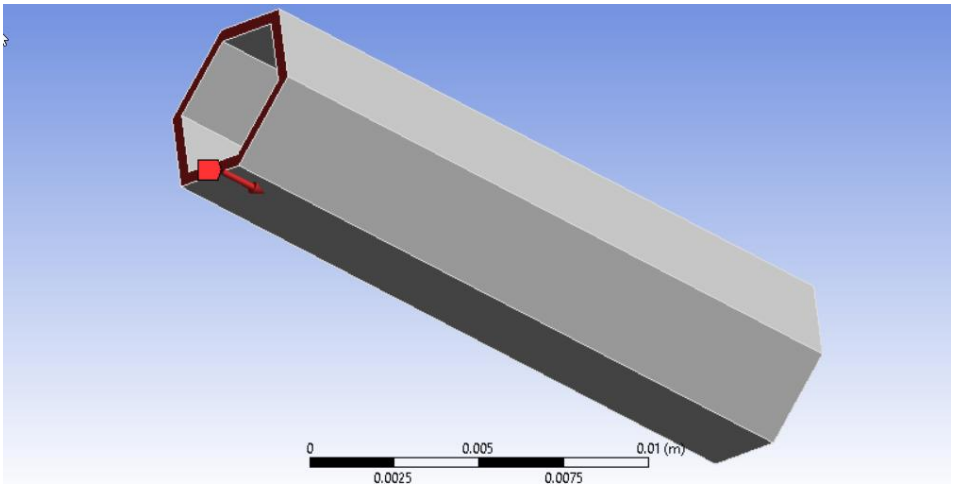


Fig 2.15 Boundary conditions for the single cell

The effect of a number of elements on the core depth has been showing in the tabular form and we also see that the elements have been increased with the increase in mesh sizes and the size of the honeycomb structures. In this study, we have used 3,5,10mm cell wall length to determine the behavior of the honeycomb structure based on the increase in the length and effect on it. The study shows that the deformation is more seen in the 3mm cell length and it increases steadily with the increase of the load and we see similar results for the remaining 5 and 10mm, with the cell wall length increase the buckling strength increase and the energy absorption also increase with the increase of the cell wall length.

If we look at the graphs plotted for the various mesh sizes vs total deformation, von-misses stress and strain energy and the data obtained from mesh independence study show that with the increase in cell length the percentage of error is keeps increasing for the 3mm and the data points show that the gap is narrowed with the increase of the cell wall length.

The real science behind of increase in cell wall length helps to prevent further buckling of the cell and the stress and deformation is peak initially and the cell resists the deformation creating the energy absorption which allows the cell to absorb more stress and avoid buckling, the loads are applied step size 5 with 1000N to 5000N. The max deformation was observed for the 3 mm and the least deformation is obtained for 5000N which is 0.000028248mm.

These structures which can be deployed in various applications based on the loading conditions, this study mainly deals with single cell honeycomb structure and then eventually taken to the chiral shapes with different geometry and boundary conditions and these shapes are build in matrix format like a sandwich structure and the analysis are also performed using SOLIDWORKS and Ansy.

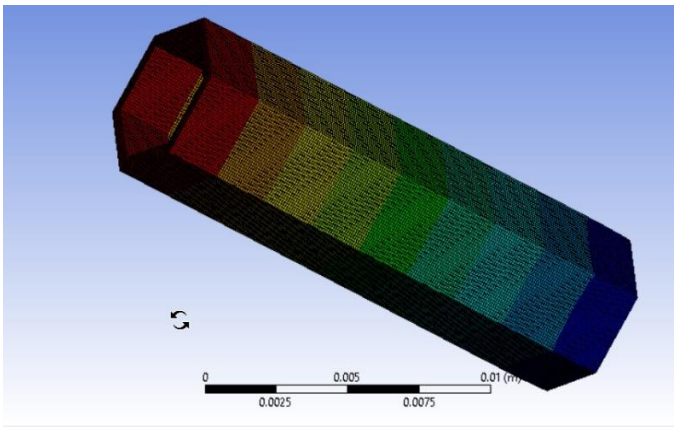


Fig 2.16 Total Deformation for 3mm cell

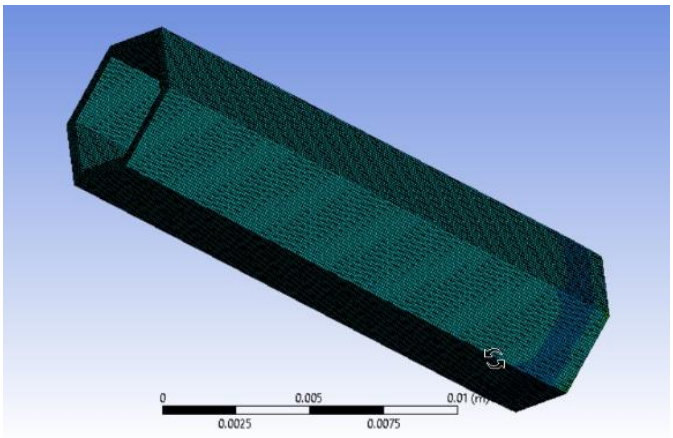


Fig 2.17 Von-Misses Stress for 3mm cell

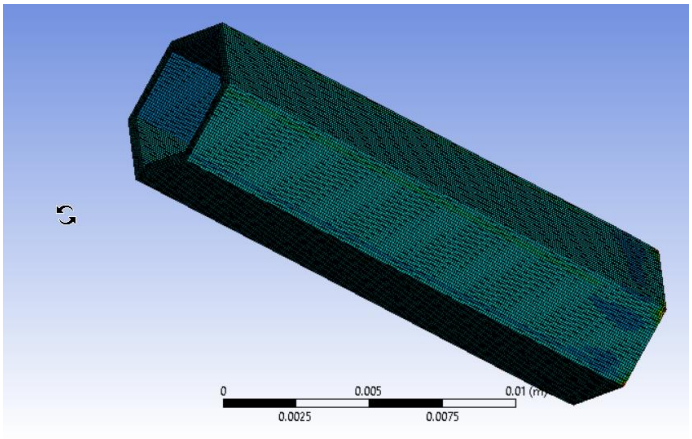


Fig 2.18 Strain energy for 3mm cell

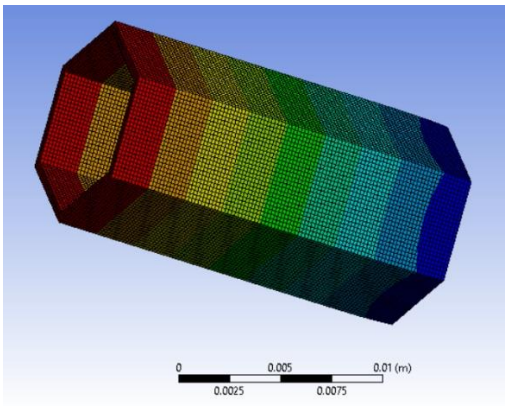


Fig 2.19 Total Deformation for 5mm cell

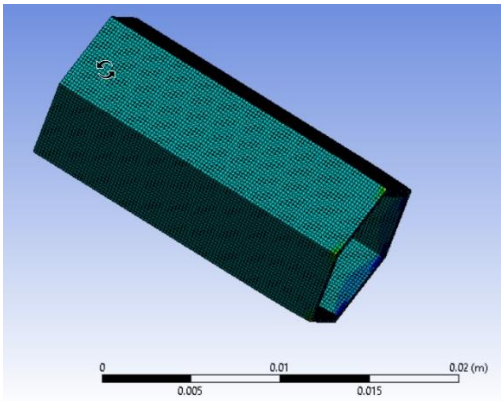


Fig 2.20 Total Deformation for 5mm cell

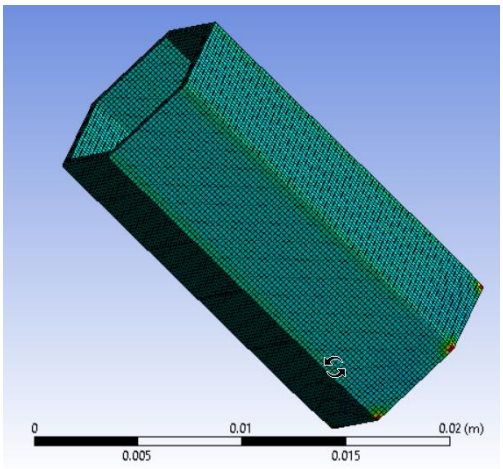


Fig 2.21 Total Deformation for 5mm cell

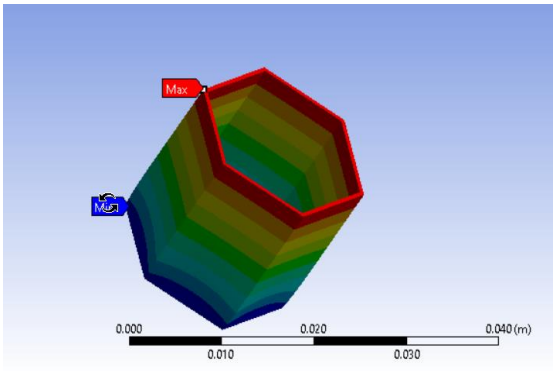


Fig 2.19 Total Deformation for 10mm cell

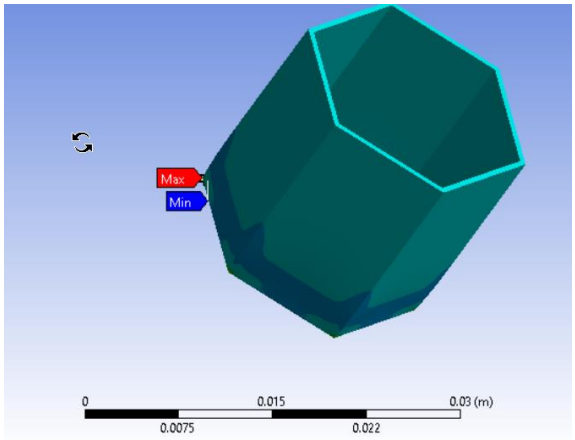


Fig 2.19 Total Deformation for 10mm cell

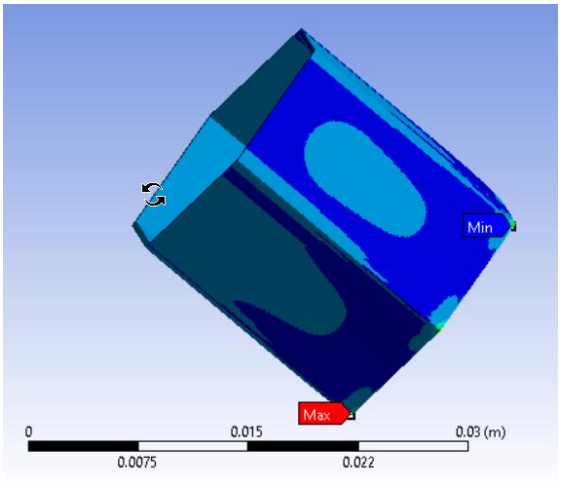


Fig 2.19 Total Deformation for 10mm cell

This study mainly gives us an insight of the behavior of cellular materials under various loading conditions and not only limited to that but also extent to modal analysis which helps us understand more even about the cell behavior under its natural frequency with the increase of the cell wall lengths and also the comparison has been studies for the different geometry shapes and chiral parts for the investigation and to determine which shape or cell is more suitable.

# Chapter 4

## Buckling and theoretical prediction of single cells and chiral honeycomb structure

When a simply supported beam, panel is subjected to in-plane compressive loads, buckling failure can occur. Usually buckling is characterized by a sudden out-of-plane deformation of the sandwich panel. Buckling also occurs even when applied in-plane loads as well. Global instability mode of a sandwich structure is commonly referred to as the overall buckling mode of the structure.

Buckling of the sandwich panel occurs I several possible modes. In one modem the face-sheet layers and the core experience the same out-of-plane deformation this mode is also knows as global buckling mode, where the deformation is like a long wavelength that is equal to the length of the flat sandwich plate. This mode is also commonly called as asymmetric buckling mode. If there is a short-wavelength buckling mode in which core material is compressed or stretched the phenomena is called symmetric buckling mode.

The overall sandwich panel deformation can be calculated and studied to determine the critical buckling load and different buckling modes to understand the phenomenon. The significant response is core stiffness an core shear strength and also the thickness and surface panel pay a key role in the analysis.

- Modal analysis is a typical starting point of dynamic analysis, it's a most fundamental of all dynamic analysis type, essentially it looks for natural frequency of the structure.
- This analysis helps us study the design response to various dynamic loads.
- Every structure exhibits its own natural frequency in which we study them to understand and design within safe range to avoid resonance which could lead to failure of the component.
- It helps us understand more complex behavior which leads to more complex dynamic simulations are based on natural frequencies.

Governing equation

$$[M]\{\ddot{U}\} + [C]\{\dot{U}\} + [K]\{U\} = \{f(t)\}$$

- Typically, we remove the loads and damping which simplifies and becomes free and undamped vibration system.

$$[M]\{\ddot{U}\} + [K]\{U\} = 0$$

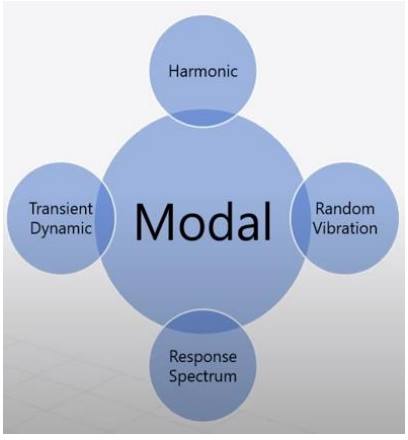


Figure 3.1 Modal of the buckling

- Buckling happens when compressive load is applied and also point of interest is studying the point of buckling.
- Buckling is not due to inertial force, in fact its' due to sudden change of its potential energy of the system into kinetic energy.
- So the governing equation starts with just the stiffness equation.

$$[M]\{\ddot{U}\} + [C]\{\dot{U}\} + [K]\{U\} = \{f(t)\}$$

$$[K]\{U\}$$

- We use non-linear analysis because of static problem and being our objective of study.

when a load is applied the equations changes to $[K]\{U\} - \{F\} \neq 0$

- The results obtained are very accurate compared to linear analysis.
- For out of plane deformation Gibson and Ashby have derived a formula for $P_{cr}$

$$P_{cr} = \frac{KE_s}{(1-\nu^2)}\frac{t^3}{l}$$

K = constraint factor, l= cell length and t = thickness of cell wall

When simply supported sandwich, panel is subjected to in-plane with compressive loads, and the buckling failure can occur. Buckling is characterized by a sudden out-of-plane deformation of the sandwich pane. Buckling may occur even when the applied in-plane loads are well below the failure loads for the material out of which the sandwich structure is made.

Buckling of the sandwich panel has many possible ways in which one mode, the face sheet layers and the core experience the same out-of-plane deformation this mode is known as global buckling mode. In this the deformation is like a long wavelength that is equal to the length of the flat sandwich plate and the other mode of possible is short wavelength mode which is face-sheet and the core layer do not extend laterally to the thickness of the intermediate layer. This type is more common also called an asymmetric buckling mode, and the other one where the core material is stretched or compressed is called a symmetric buckling mode.

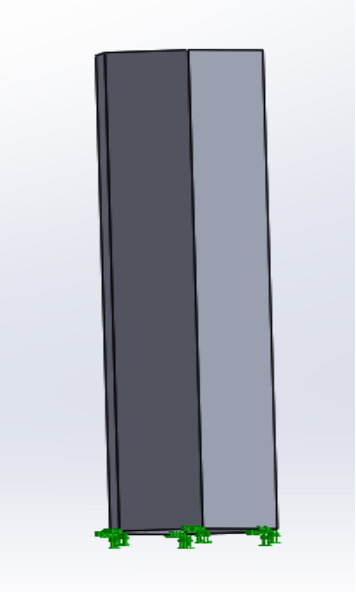

Figure 3.2 Modal of the cell

Finite Element modeling of sandwich single-cell structures or panel have many approaches and can be used in different manner, but we narrow it to on kind depending on the panel geometry and material properties. The three main approaches are fully shell, shell/solid element and three-dimensional solid element model. The buckling behavior of a sandwich panel depends on te sandwich panel geometry and material properties. It involves general instability mode and a local instability mode or both. The precise prediction of the overall buckling modes of a sandwich panel requires adequate representation of the sandwich stiffness and the prediction of wrinkling mode requires the thickness of the model.

The first method helps us in shell finite elements. These modes are also conventional shell elements. The sandwich shells provide a good approximation of the global buckling and wrinkling behavior.

The second method uses conventional shell finite element methods for the face sheet and solid three-dimensional finite element behavior. These models are conventional a used in SOLIDWORKS and ansys for the accuracy.

The third method is full three-dimensional finite element mode, in which full solid elements are used to model both the face-sheets and the core material. The third approach is also known as full three-dimensional solid element models in Abaqus/CAE software. They are used where the models are carried and has no limit with computational cost.

- The honeycomb fails by uniaxial yield which is given by $(\sigma_{pl})_3 = \sigma_{ys}(\frac{\rho^*}{\rho s})$

- Gibson and Ashby calculated that the plateau stress for the compressive strength is given by.

$$(\sigma_{pl})_3 = \frac{\pi}{4}\,\sigma_{ys}\,(\frac{t}{l})^2\,\frac{(\frac{h}{l}+2)}{(\frac{h}{l}+sin\theta)cos\theta}$$

- For regular hexagon $(\sigma_{pl})_3 \approx 2\,\sigma_{ys}\,(\frac{t}{l})^2$ the exact calculation is $(\sigma_{pl})_3 = 5.6\,(\frac{t}{l})^{\frac{5}{3}}$

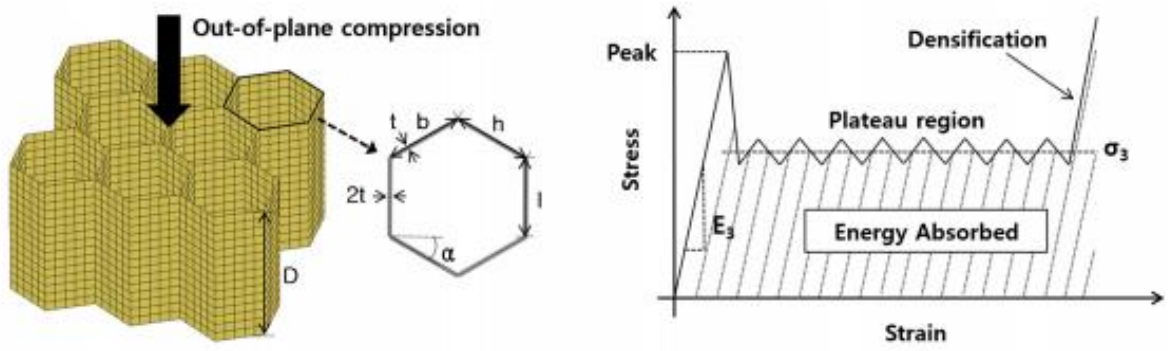


Figure 3.4 Out-of-plane of honeycomb structure

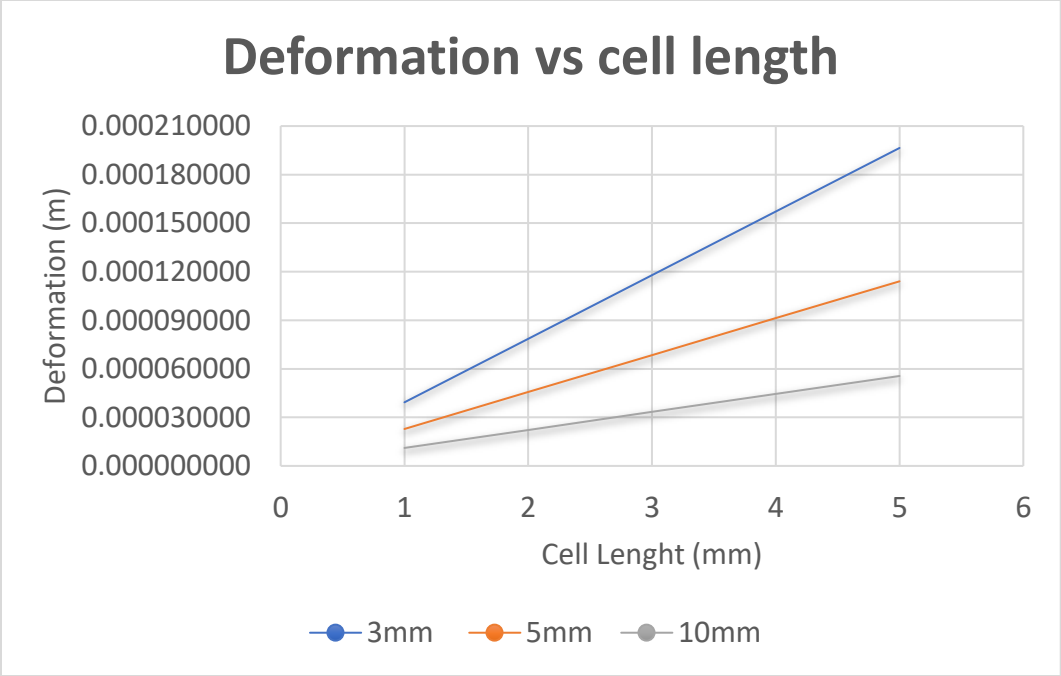


Fig 3.3 Comparison of deformation vs cell length

The graph explains more of the deformation of the sandwich structure based on the varying cell length and we observe that the deformation keeps increasing with the increase in load and the cell length play a significant role as we can see that the deformation is controlled and constrained with the cell length increase. The 10mm cell length has shown a significant tolerance to deformations and resistance to load carrying capacity. sss

Since the cell wall length with the large length tend to absorb loading and would prevent the structure from buckling. The honeycomb structure has shown a significant decrease of the deformation with the increase in the cell length and it help us to understand the dynamics of the sandwich structures.

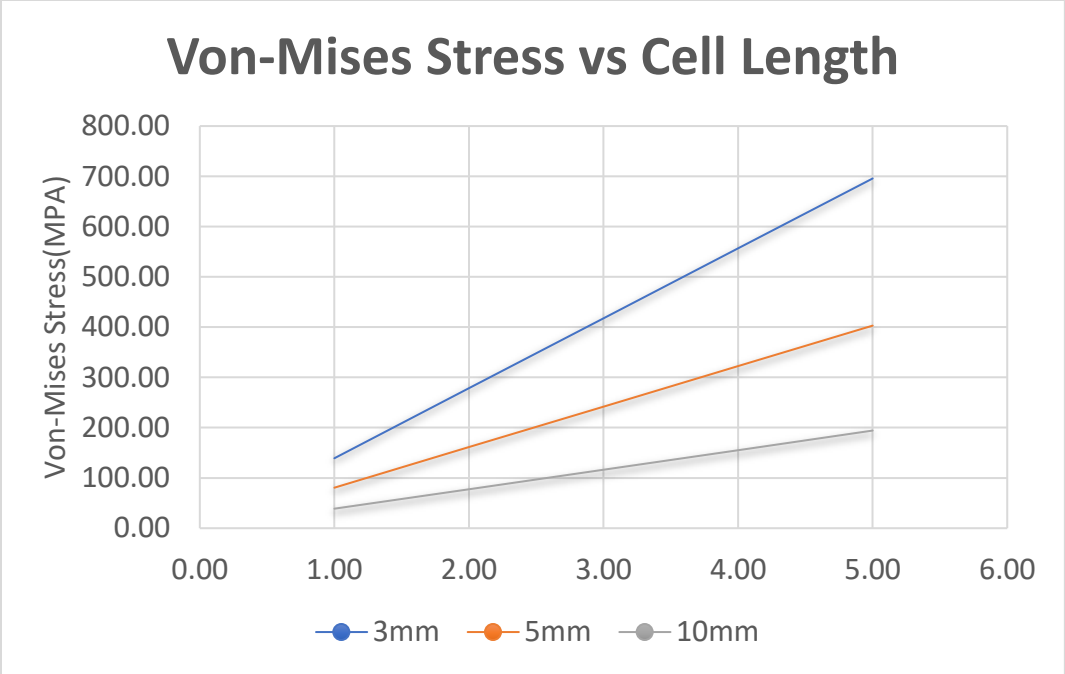


Fig 3.5 Comparison of the von-misses vs cell length.

The von-mises stress of the honeycomb structure are shown in the fig which explains the stress for the various cell wall length and we can see from the graph the von-mises stress is higher for the 3mm and the least was seen for the 10mm cell wall length. We can make the conclusion that the higher the cell wall length we can see the more tolerant for the stress and they are more least susceptible to failure.

The stress induced by the structure for each cell is different and the amount of stress for the 3mm cell length is the highest and the 10mm is the more stable and shows a greater resistance to the deformation.

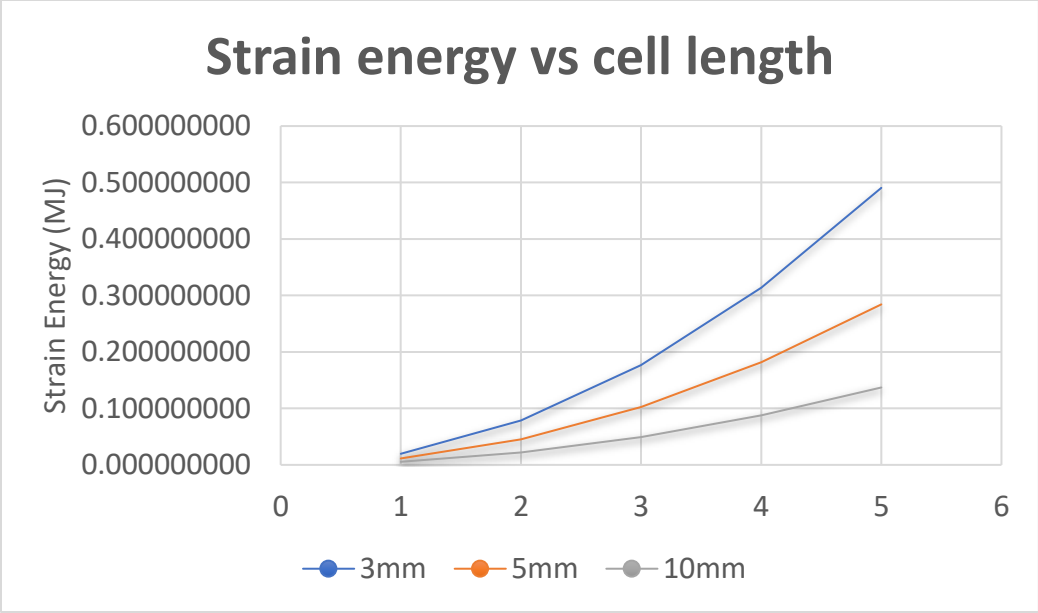


Fig 3.6 Comparison of strain energy vs cell length

The strain energy is nothing but the potential energy that is stored in a structure member as a result of elastic deformation, we use the determination of strain energy because to quantify the effect of residual stress on mechanical behavior. In the graph plotted we can clearly see that the highest strain energy is obtained by 3mm and the least is observed for 10mm.

With the increase in the cell length the strain energy decreases and potential to store for the elastic deformation is greater and seen for 3mm cell length, for the application based 3mm is more suitable for the energy absorption.

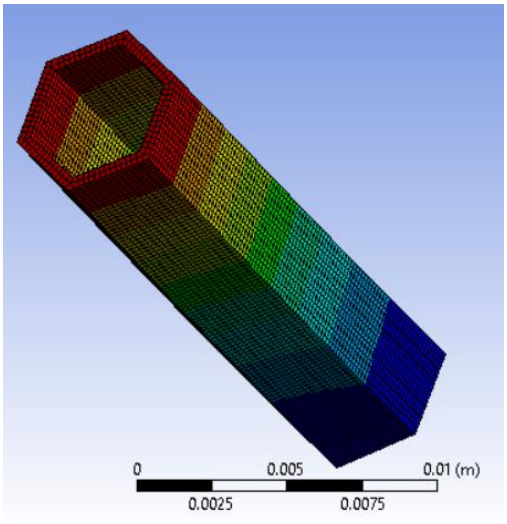


Fig 3.7 Mode shape 1- 3mm

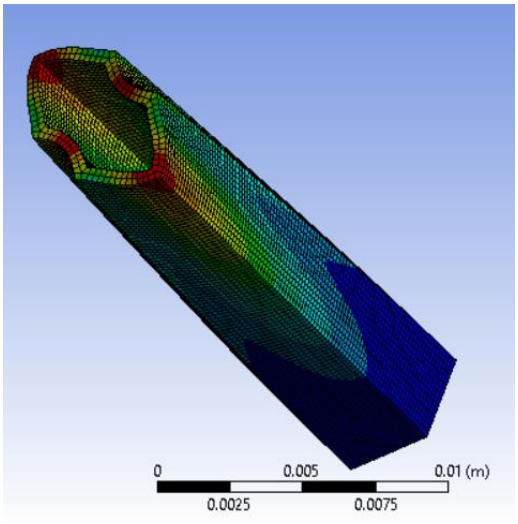


Fig 3.8 Mode shape 2 - 3mm

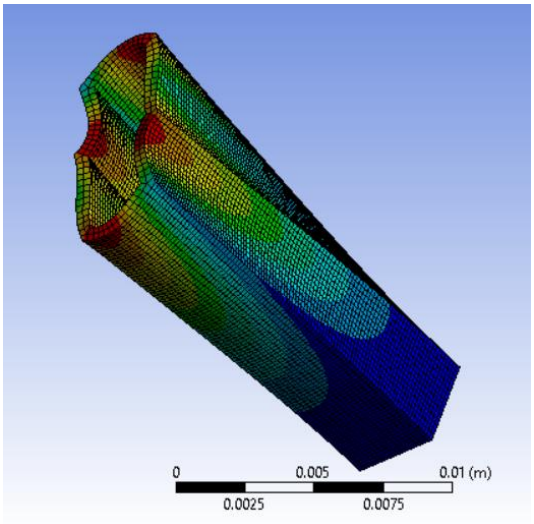


Fig 3.9 Mode shape 3

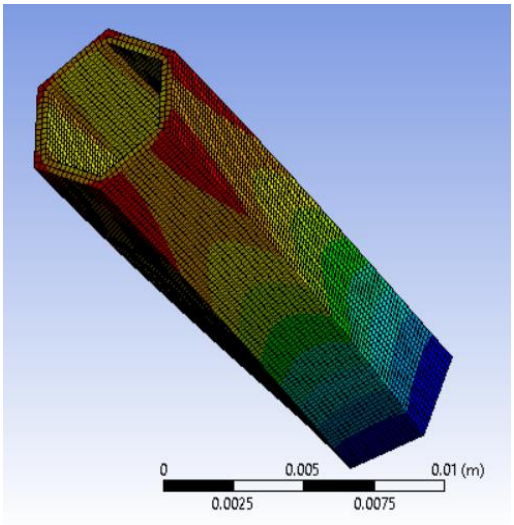


Fig 3.10 Mode shape 4

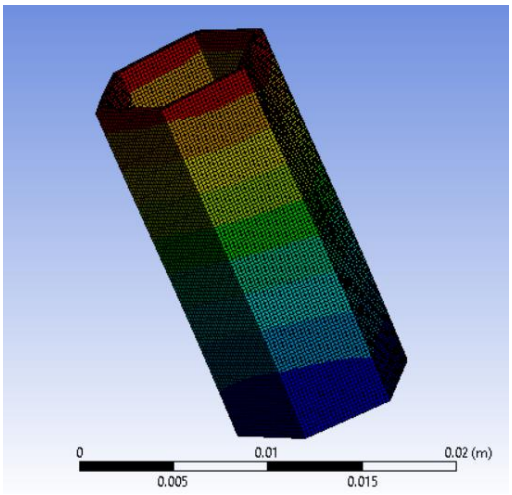


Fig 3.11 Mode shape 1 of 5mm

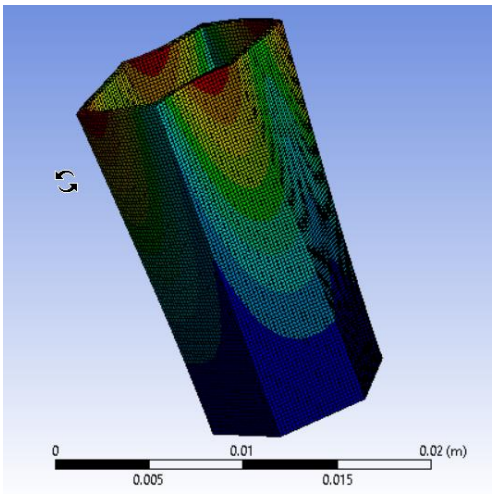


Fig 3.12 Mode shape 2 of 5mm

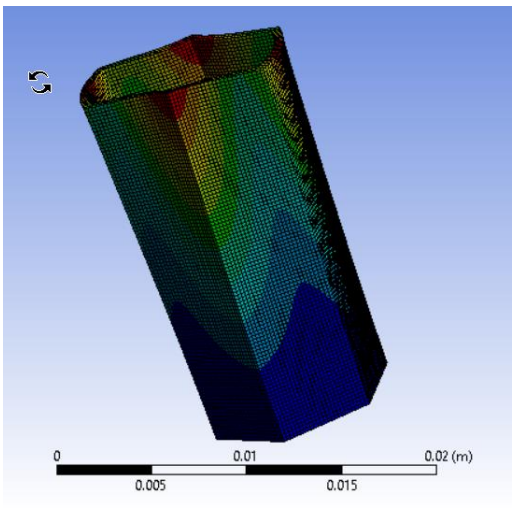


Fig 3.13 Mode shape 3 of 5mm

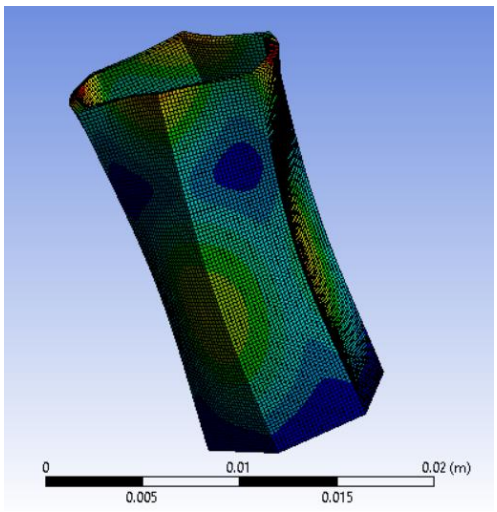


Fig 3.14 Mode shape 4 of 5 mm

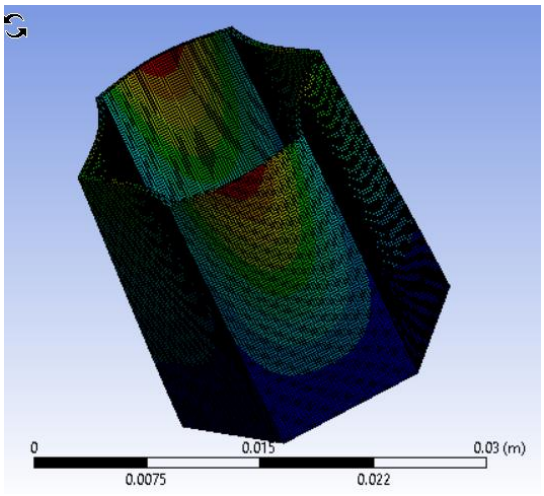


Fig 3.15 Mode shape 1 of 10mm

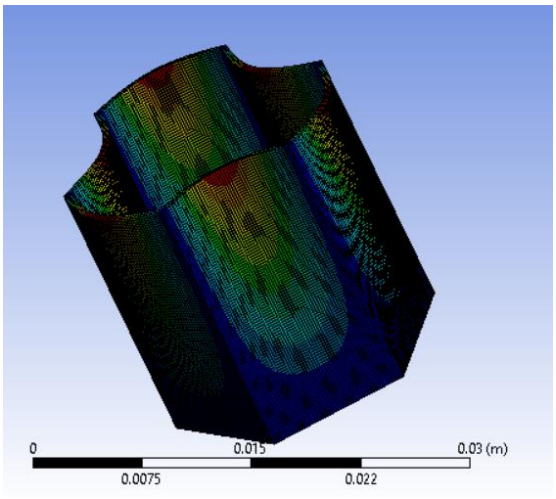


Fig 3.16 Mode shape 2 of 10mm

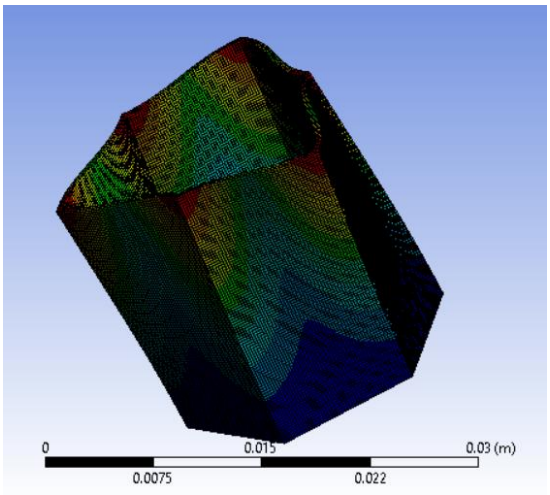


Fig 3.17 Mode shape 3 of 10mm

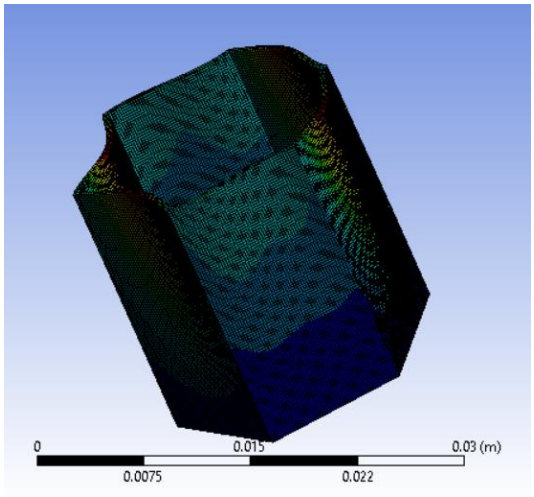


Fig 3.18 Mode shape 4 of 10mm

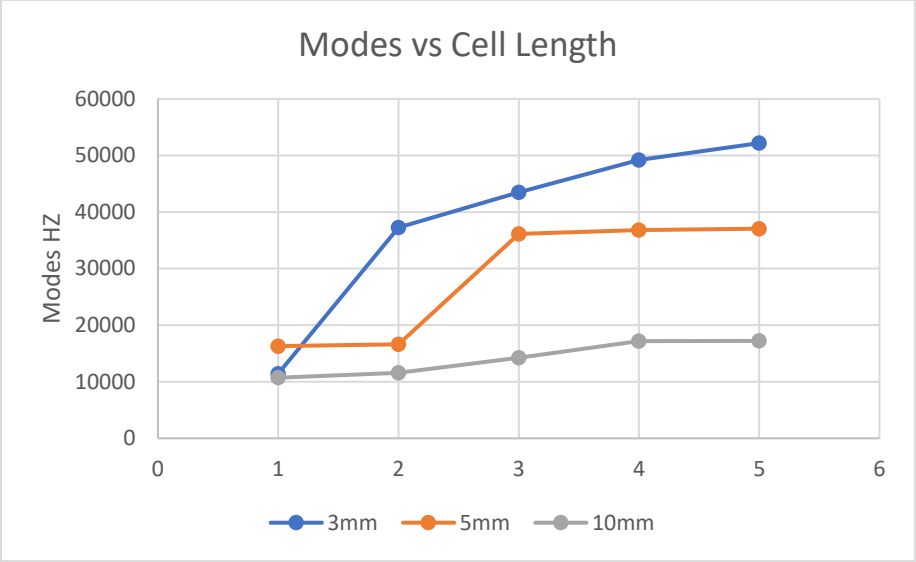


Fig 3.19 Mode vs cell length of various sizes.

The modes are nothing but the frequencies of the cells under natural and we can see that the 3mm cell has the increment of the frequencies for the first 5 nodes and the 5mm has slightly higher than the 3mm and which increases to certain amount and then remains constant and stable. The effective orthotropic properties of honeycomb core can be measured experimentally or predicted using analytical or using numerical models. The homogenization of the honeycomb core and determining the effective mechanical properties have been investigated and the node and frequency are evaluated to study the behavior of the cell under natural frequency.

| Cell Length | Mode1 (Hz) | Mode 2 (Hz) | Mode 3 (Hz) | Mode 4(Hz) | Mode 5 (Hz) |
|---|---|---|---|---|---|
| 3mm | 11429 | 37272 | 43482 | 49211 | 52178 |
| 5mm | 16304 | 16639 | 36123 | 36814 | 37060 |
| 10mm | 10713 | 11608 | 14249 | 17210 | 17222 |

Table. 3.20 Mode shapes and cell length

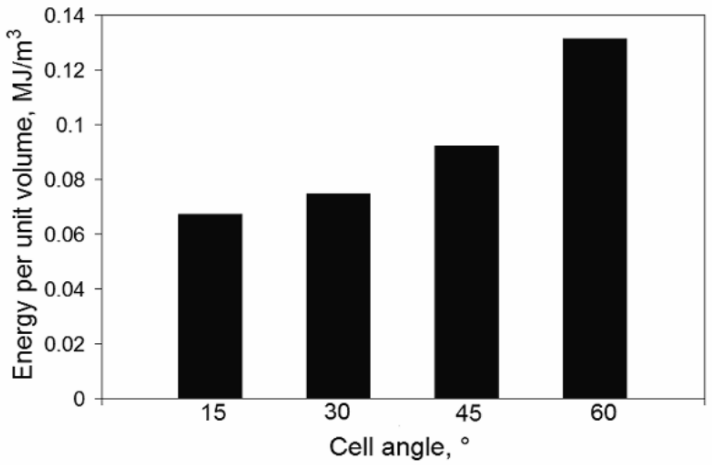


Fig 3.21 Graph showing cell angle vs energy per unit volume.

The cell angle for the honeycomb structure plays an important role based on the application for the various structures. The cell angle is nothing but the angle between two adjacent walls of the structure and it can be varied, and the study or comparison is compared among the various cell geometry. We can see that $15^0$ has the lowest energy per unit volume (MJ/$m^3$) and the cell angle $60^0$ has the highest energy per unit volume as the cell wall angle increases the energy per unit volume also increases and which helps the structure to be stable.

Deformed and undeformed honeycombs that are observed under buckling and we can see that $60^0$ honeycomb develop much more bending than the $15^0$ honeycomb and the rest of the inclines wall rotates around it. The inclined walls they don't behave as a rigid body undergoing pure rotation around the hinge.

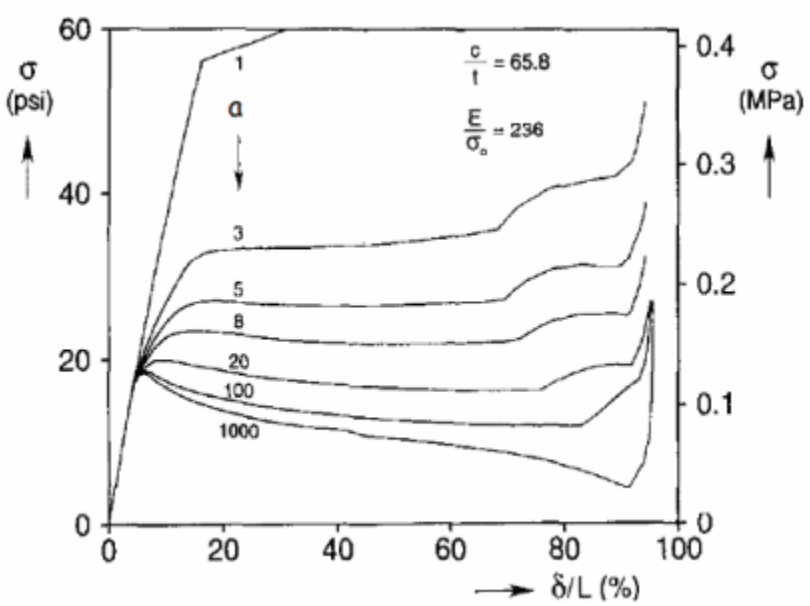


Fig 3.22 graph plotted between stress and the strain

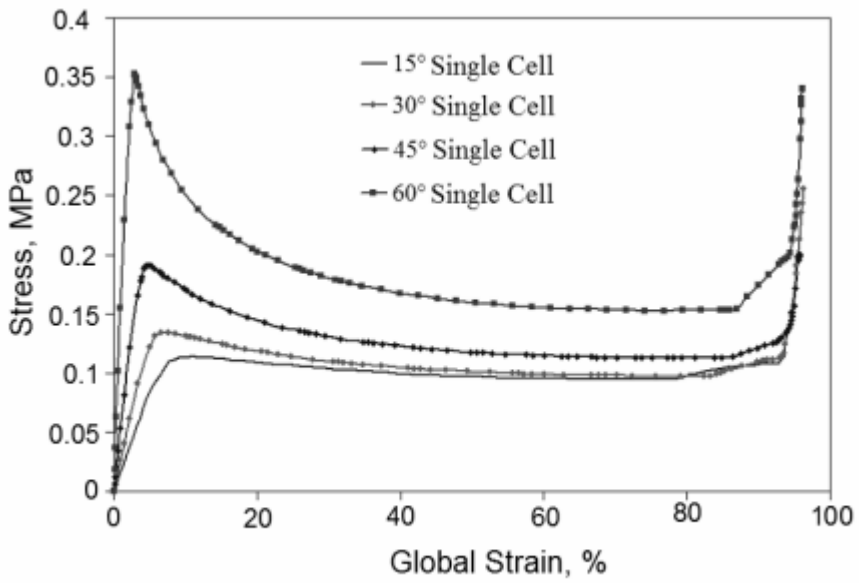


Fig 3.23 graph plotted between global strain vs stress

Sandwich Honeycomb structures are nothing, but composite materials made up of two or more components, they have a core and face sheets, the core is at the center and the face sheets are placed one from the top and the other one at the bottom and then sandwiched together making a strong joint for various applications. The global strain of the first cell angle is more peak for the stress and there is a sudden decline.

Honeycomb sandwich panels are being used in various application starting from aerospace to medical devices and there are used in almost every structural material to reduce weight and increase the strength. Sandwich panels have become more and more common in different engineering structure, including aircraft. Compared to metal plates or composite laminates, the sandwich structure has interesting characteristics such as a high-energy absorption capacity and high flexural stiffness.

Sandwich panel consists of a porous low-density core, honeycomb or foam and two stiff metal or composite faces. The sandwich panels usually absorb impact energy which uses two different mechanism, namely local crushing and global bending. In crushing mode, the low-density core under the point of impact is crushed mode, the low-density core under the point of impact is crushed to great extent and absorbs significant amounts of energy by plasticity of the walls. In the global bending mode, the whole structure bends and absorbs energy by plastic deformation of the structure.

Due to the relatively large distances of the faces, the moment of inertia of the sandwich panel is relatively high, which increases the flexural stiffness of the sandwich panel as well. High flexural stiffness of the whole sandwich panel and a high flexibility of its core material yield a high-energy absorption capacity of the sandwich structure which is very suitable for high-energy impacts, such as bird strike. The core material must have increased shear strength to prevent relative sliding of the sandwich faces in a bending deformation. In addition, the core material must have some degrees of stiffness to ensure its flatness at its interfaces with the skins and to avoid wrinkling of the intact regions of the skins during an impact process.

Honeycomb structures with panel.

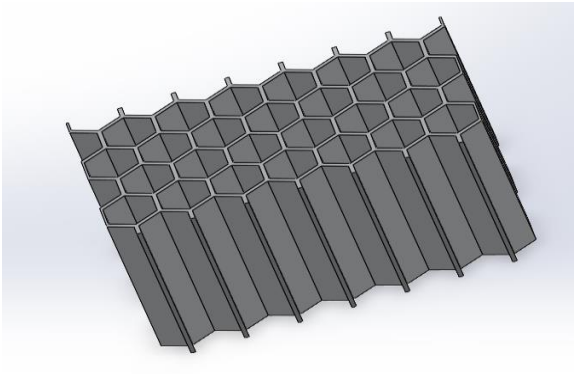

Fig 3.24 Model of honeycomb 4x6 panel 3mm

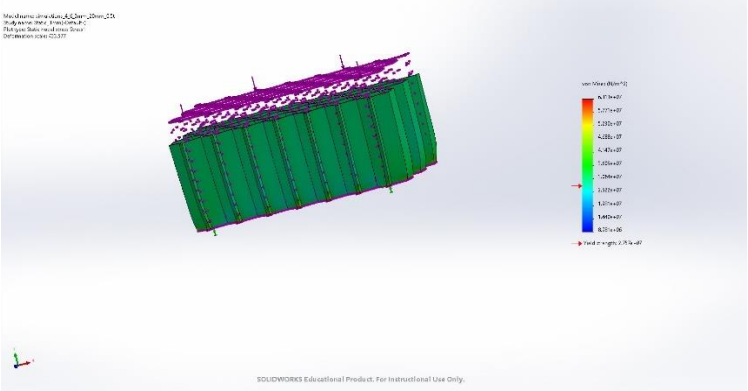

Fig 3.25 Equivalent stress of honeycomb 4x6 panel 3mm

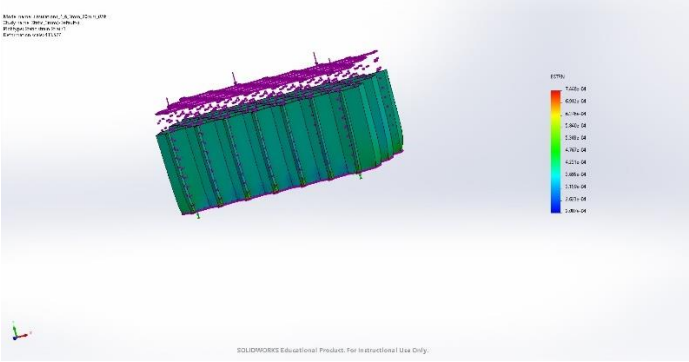

Fig 3.26 Total Deformation of honeycomb 4x6 panel 3mm

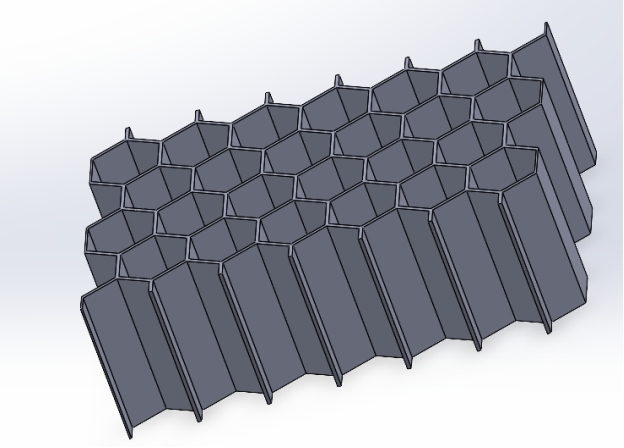

Fig 3.27 Model of honeycomb 4x6 panel 5mm

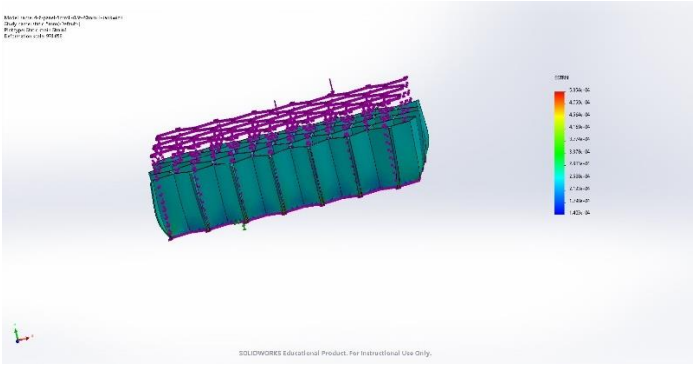

Fig 3.28 Equivalent Stress of honeycomb 4x6 panel 5mm

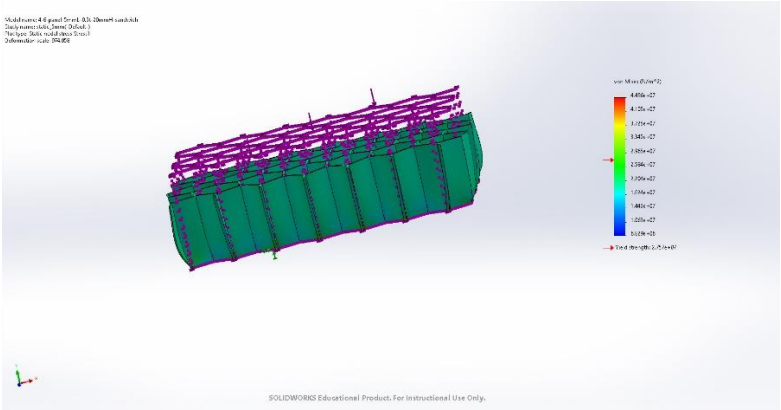

Fig 3.29 Total Deformation of honeycomb 4x6 panel 5mm

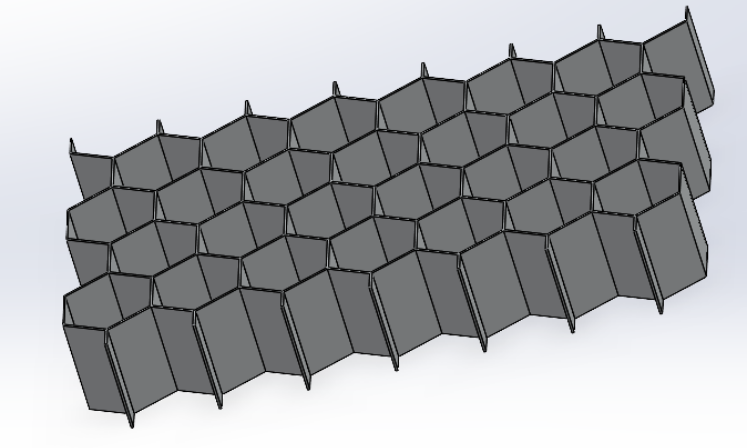

Fig 3.30 Model of honeycomb 4x6 panel of 10 mm

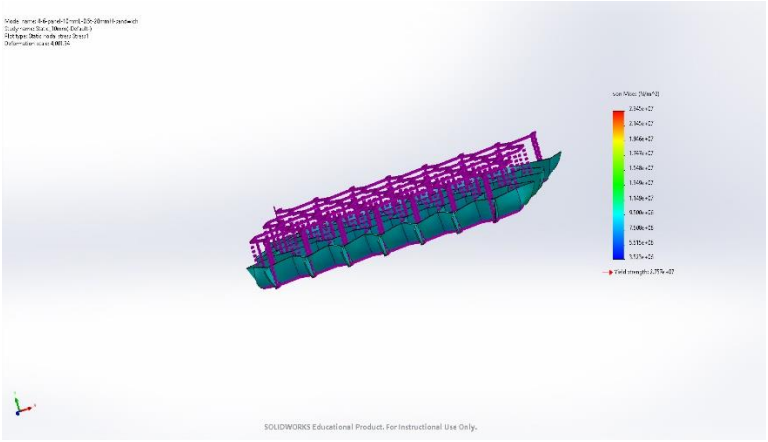


Fig 3.31 Equivalent stress of 4x6 panel of 10mm

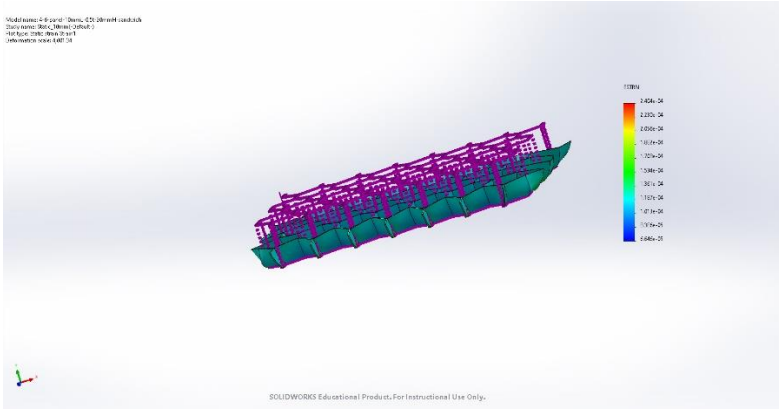


Fig 3.32 Total Deformation of 4x6 panel of 10mm

# Chapter 5

## Chiral Honeycomb structures

Low-density cellular solids have demonstrated superior mechanical properties as well as multifunctional characteristics, which may provide different multifunctional characteristics, which may provide basis for the development of novel structured materials called as chiral shapes or chiral honeycomb structures.

While the stochastic configurations such as metallic foams have proven to be more effective for both thermal and mechanical-energy absorption. The topology of deterministic architectures is not constrained by physical processes and tailored to simultaneously fulfill disparate tasks. This allows the variety of configuration and provide and new opportunities in the fields of structural dynamics, where periodically-inducted impedance leads to the control of both constructive and destructive interference on propagating waves.

The objective of this work is to investigate the application of the chiral cellular topology for the design of novel macrostructural, mesostructured and microstructure. An important aspect of deterministic cellular configurations is the possibility of assembling materials or structures, by the spatial repetition of a unit cell. The resulting periodicity of such systems simplifies the characterization of physical properties.

- Chiral shapes are man-made solids designed to exhibit negative Poisson's ratio.
- In this presentation we are trying to emphasize more on the chiral shapes and study the behavior of the chiral lattice and its applications.

- Metallic foams and re-entrant cellular solids have contributed significant applications compared to conventional honeycomb and the properties have consistently shown dominating in stress resistant and the energy absorption.
- Chiral/Auxetic materials have interest have a counterintuitive behavior under strain and enhanced strength, better acoustic behavior and improved fracture toughness.
- This Auxetic honeycomb as core material in curved body not only showed out-of-plane properties to be superior in bending and also high stiffness.
- The hexagonal honeycomb has the attribute of lattice with six-fold geometric symmetry in the plane, while the chirality has the topology of non-invariant to reflections.
- Significant advancements in material science have established both the occurrence and the practicality of chiral shape solids.

Mechanics of Chiral honeycomb structures

- The hexagonal chiral lattices in general consists of circular elements of radius r, which are connected by ribs or also called as ligaments of length L and the distance between each node is R, wall thickness is $t_c$.

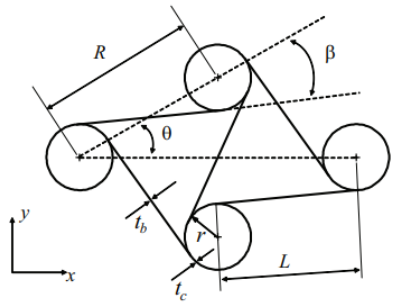


Fig 4.1 Mode of chiral shape 1

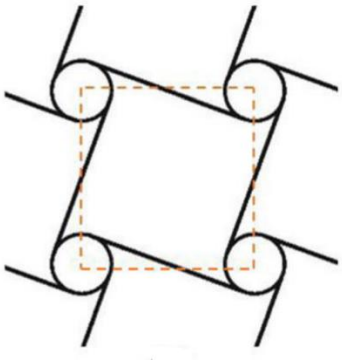

Fig 4.2 Model of chiral shape 2

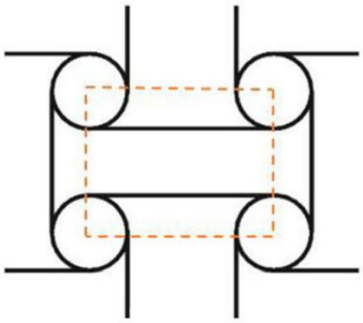

- Sinβ = $\frac{2r}{R}$ tan β = $\frac{2r}{L}$, and sin β = $\frac{L}{R}$
- The L/R ratio yields significantly depending on the geometry.
- The geometry parameters remain same but the orientation is the only which differentiates the geometries.
- The angle θ is always 30◦ which states the hexagonal chiral topology is invariant to in-plane rotations by 2θ.
- Since the influence of hexagonal symmetry of the mechanical behavior results in-plane isotropy.
- The young's modulus of hexagonal material is independent of the plane normal to the hexagonal symmetry axis
- The chiral-core honeycombs are generally expected to transversally-isotropic components.

$$\epsilon = \begin{bmatrix} \frac{1}{E_x} & \frac{-U_{xy}}{E_x} & \frac{-U_{xz}}{E_z} & 0 & 0 & 0 \\ \frac{-U_{xy}}{E_x} & \frac{1}{E_x} & \frac{-U_{xz}}{E_x} & 0 & 0 & 0 \\ \frac{-U_{xz}}{E_z} & \frac{-U_{xz}}{E_z} & \frac{1}{E_z} & 0 & 0 & 0 \\ 0 & 0 & 0 & \frac{1}{-G_{yz}} & 0 & 0 \\ 0 & 0 & 0 & \frac{1}{E_x} & \frac{1}{G_{yz}} & 0 \\ 0 & 0 & 0 & 0 & 0 & \frac{2(1-U_{xy})}{E_x} \end{bmatrix} \boldsymbol{\sigma}$$

Fig 4.4 Orthotropic properties of honeycomb structure

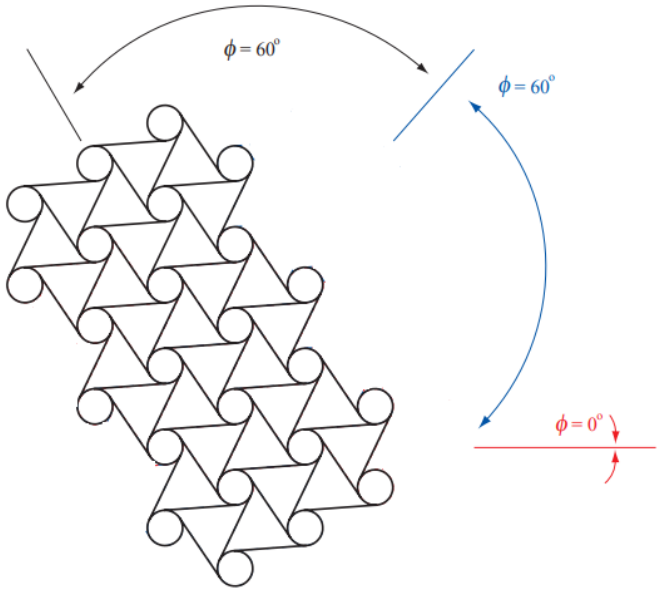


Fig 4.5 Loading characteristics of honeycomb structure

- The mechanical behavior of the hexagonal chiral lattice is strongly dependent upon the wall thickness of the lattice's components, it also helps us to understand and study static and dynamic responses of chiral assemblies.

- In general, relative density $\bar{f}$ of two-phase composite is nothing but the volume occupied by one phase, in this case the walls of a unit cell, normalized by the sum of the volumes of the both phases.

$$\bar{f} = \frac{f^*}{f_S} = \frac{2\pi r t_c + 6 L t_b/2}{R^2}$$

$f^*$ = equivalent density of the lattice, $f_S$ is the constituent material. The wall thickness of the model $t_c$ and the ligament thickness is given by $t_b$.

- Negative Poisson's ratio materials exhibit very unique mechanical behavior, transversally expanding when stretched and transversally contracting when compressed and such materials are called auxetic.

In-Plane behavior:

- chiral honeycomb has a strong influence on L/R ratio, the large global deformation within the elastic regime of the constituent material.
- The assessment of in-plane mechanical properties is based on applying equilibrium of externally applied stresses with resulting internal forces on a unit cell.
- Assuming the nodes to be perfectly rigid and neglecting shear and axial deformation.
- Let's say P, W and M are reactant forces applied in the transverse direction and W is reactant force applied in the longitudinal direction, M represents the moment.
- The moment M is given by

$M_x = \frac{PLsin(\theta-\beta)}{2}$

X- direction of externally applied stress.

- Since it's a static equilibrium, W is Zero
- No applied stresses in the y-direction.

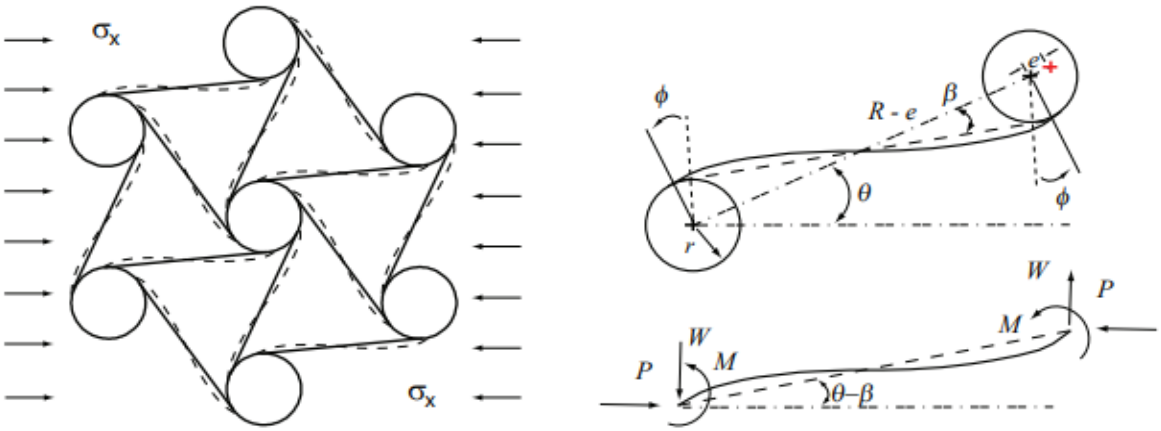


Fig 4.6 In-Plane loading properties of honeycomb structure

- The same deformation is applied for $\sigma_y$, resultant force P is zero since there is no applied stress in x-direction. $M_y$ =- $\frac{WLcos(\theta-\beta)}{2}$

- Quasi-static deformation is

$U_{rib}$ = $2\int_0^{\emptyset} M(\emptyset^{/})d\emptyset^{/}$ , due to the symmetry of the chiral lattice with period $2\theta$ ($60^0$)

- If bending deformation is considered, the relationship between end reactant moments M and end rotations $\emptyset$

$\emptyset = \frac{ML}{6E_sI}$ , I = $\frac{bt_b^3}{12}$

- $\in_x = \frac{r\emptyset cos\theta}{Rcos\theta}$ , $\in_y = \frac{r\emptyset sin\theta}{Rsin\theta}$ , Simplifying the strain equations give us

- $\in_x = \in_y = \frac{r\emptyset}{R}$ , after applying the definitions for $\vartheta_{xy} = \vartheta_{yx}$ = - $\frac{\in_x}{\in_y}$ and - $\frac{\in_y}{\in_x}$

- $\vartheta_{xy} = \vartheta_{yx} = -\frac{\frac{r\emptyset}{R}}{\frac{r\emptyset}{R}} = -1$ In-plane shear modulus is given by $G_{xy} = \frac{E_x}{2(1+V_{xy})}$

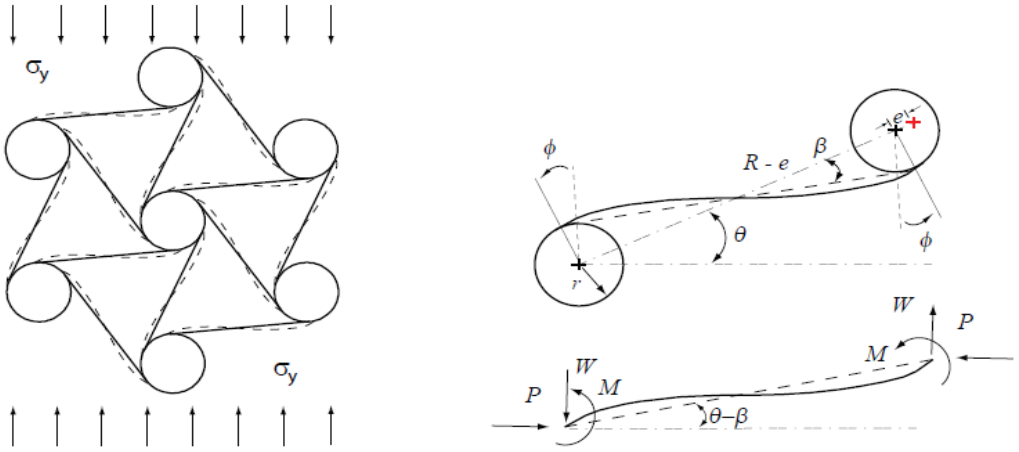


Fig 4.7 In-plane loading properties of honeycomb structure

Out-of-plane deformation of chiral honeycomb structures.

Auxetic Chiral Honeycomb:

- The chiral cell geometries display the counter-intuitive of exhibiting negative Poisson's ratio, that is when expanded laterally when stretched or pulled longitudinally.
- Chiral structures display rotational, but not reflective symmetry, which means they cannot be superimposed upon mirror image.
- The use of a combination of cylinders and ribs provides the possibility of partially decoupling the out-of-plane shear and compressive loading because the cylinders provide enhanced compressive strength, while the ligaments resist shear, enabling the tailoring of honeycomb sandwich cores to specific applications.

- Auxetic honeycomb structures are proposed because they display high in-plane shear stiffness and synclastic curvature, that is they form domes rather than having saddle structures.
- Chiral honeycombs have a optimized mechanical and di-electric properties and in the adaptive or deployable structures.
- These structures deform with an inherent handedness and undergo a rotative deformation under axial loading, and they rotate when loaded in compression or tension

- To determine the out-of-plane properties of chiral honeycomb prior to that we have made some assumptions

the cell wall mainly f,g and h are included in the analysis, strain energy only accounts for shear deformation

and bending of walls is neglected. t/L is small and b/L is large.

- Out-of-plane young's modulus $E_z$ is estimated by considering stress-strain

relationship for an elastic continuum, loading in Z-direction the stress is

given by $\sigma_z = E_z \in_z$, the stress acting on the area occupied by unit cell $\sigma_z = P/A$

- $P = E_s A_w \in_z = E_s (2\pi r + 3L)t \in_z$ ,$A_w$ is the surface provided by the honeycomb

walls.

- The resulting equivalent stiffness in the z-direction is then

$$\frac{E_z}{E_s} = \frac{2\sqrt{3}(2\pi r + 3L)t}{3R^2} = \frac{\rho^*}{\rho_s} = \bar{\rho}$$

- The loaded Area A = $R^2\cos\theta$

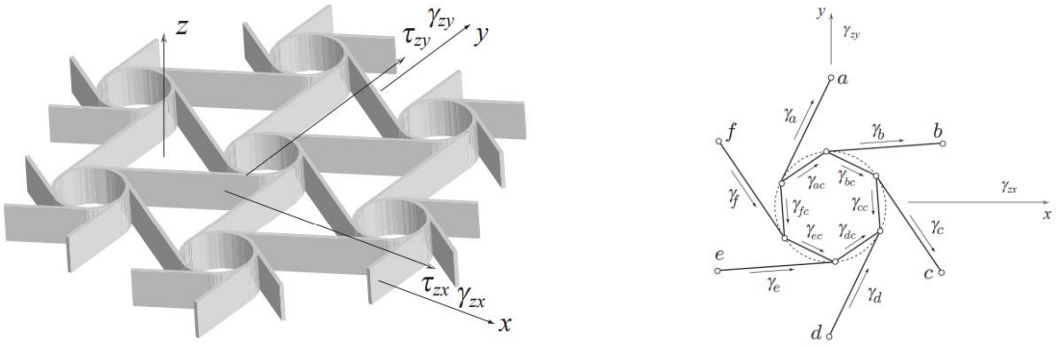


Fig 4.8 Orthotropic properties of honeycomb structure

Mesh independent study

Mesh study is conducted for a single chiral shape and we haven chosen multiple mesh sizes and the values for the elements, nodes and stress vs deformation as tabulated and compared for the best optimizing and required for the simulation and the results are very accurate and the percentage of error was within the range.

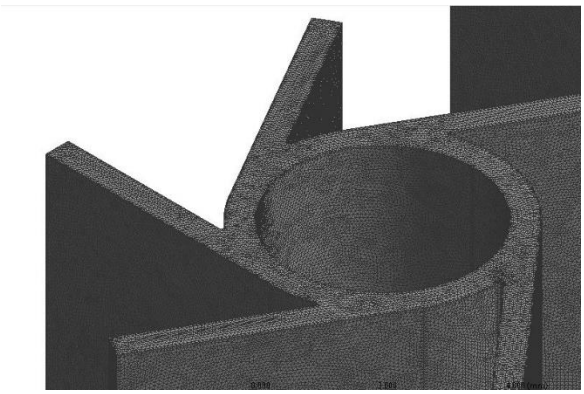

Fig 4.9 Mesh properties of chiral honeycomb structure

| MESH SIZE (MM) | ELEMENTS | NODES | EQV. STRESS (PA) | TOTAL DEF (MM) |
|---|---|---|---|---|
| 0.5 | 44366 | 78958 | 780.61 | 7.63E-08 |
| 0.25 | 120553 | 206610 | 1029.866 | 7.63E-08 |
| 0.125 | 357609 | 616870 | 1364.062 | 7.63E-08 |
| 0.0625 | 1317035 | 2256945 | 1796.55 | 7.63E-08 |
| 0.03125 | 5011207 | 8522557 | 2367.69 | 7.63E-08 |
| 0.015625 | 5036047 | 8551317 | 2364.102 | 7.64E-08 |

Fig 4.10 Mesh table properties of honeycomb structure

- The mesh independent study was conducted for varying mesh sizes ranging from 0.5mm to 0.0078125 mm.
- The elements and nodes are calculated for each mesh size and therefore tabulated to check is there any convergence.
- Study shows that mesh size 0.03125mm and 0.015625mm has almost converges and the error percentage difference is also small.
- Optimizing the right mesh size is important to run the analysis and make it reasonable.
- The graph shows there is the convergence occurs at 0.03125 and 0.015625 mm.
- Equivalent stress is 2367.4 and 2364.5 Pa and the error percentage is

below the expected range.

- The increase in mesh size results in decrease of equivalent stress.
- But the accuracy of results can be manipulated when the mesh size is too big

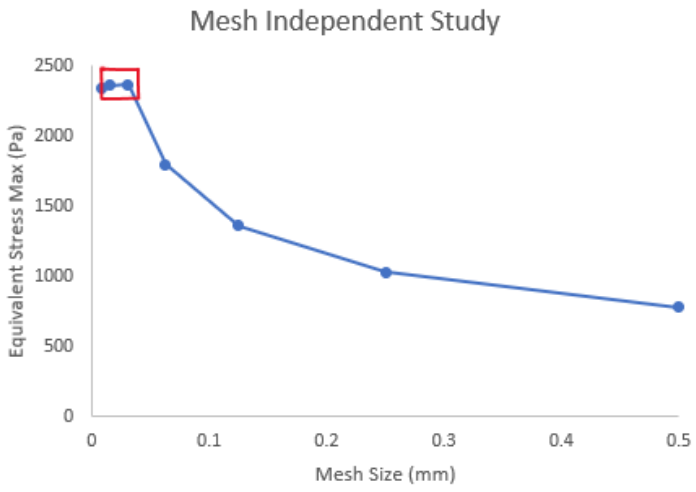


Fig 4.11 Mesh independent study of chiral structure

Auxetic chiral honeycomb

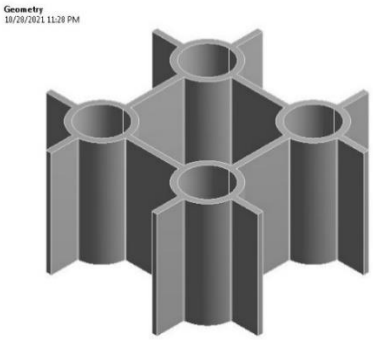


Fig 4.12 Model of Auxetic

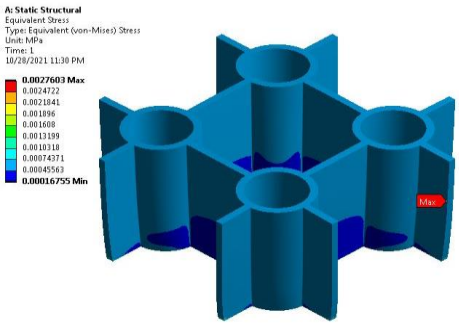


Fig 4.13 Equivalent stress of Auxetic

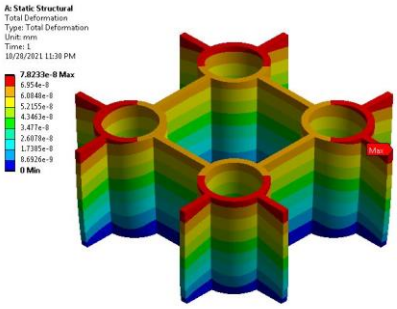


Fig 4.14 Total deformation of Auxetic

- The Auxetic Chiral Honeycomb is one of the chiral shapes used for the analysis and the ligaments or ribs are perpendicular to each other and connected to each other with the cylinder loads from 500Pa to 1500Pa are applied with intervals of 250Pa and the stress increases drastically but surprisingly we observed that the percentage of increase decreases drastically compared to 500Pa with 1250Pa from 16% to 5% with successive comparison, which shows the Auxetic chiral shape can tolerate loads and can resist buckling since the energy absorption is tremendously better than regular shape.

Anti-Chiral Honeycomb

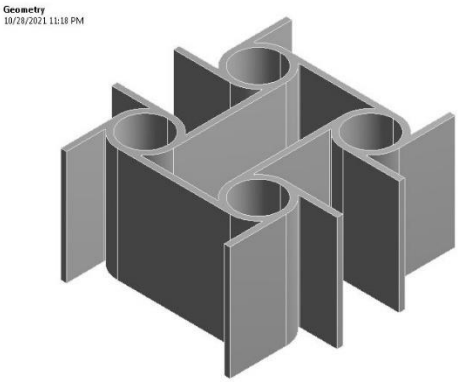


Fig 4.15 Model of Anti-chiral

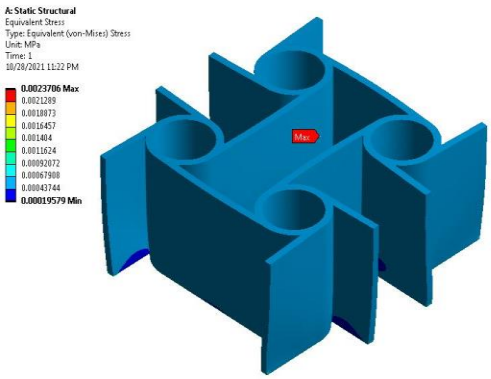


Fig 4.16 Equivalent stress of Anti-chiral

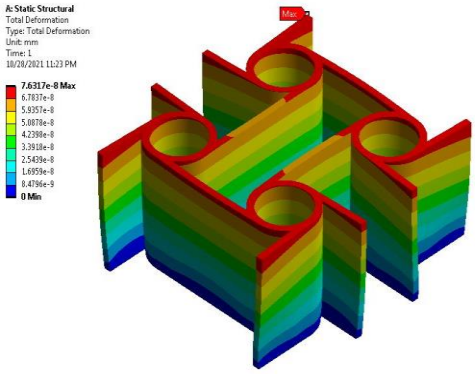


Fig 4.17 Total deformation of Anti-Chiral

- The Anti- Chiral Honeycomb is one of the chiral shapes used for the analysis and the ligaments or ribs are connected tangentially

  with the help of cylinders loads from 500Pa to 1500Pa are applied with intervals of 250Pa and the stress increases drastically but surprisingly we observed that the percentage of increase decreases drastically compared to 500Pa with 1250Pa from 17% to 5%, which shows the Anti- chiral shape can tolerate loads and can resist buckling since the energy absorption is tremendously better than conventional honeycomb.

Hexa-Chiral Honeycomb

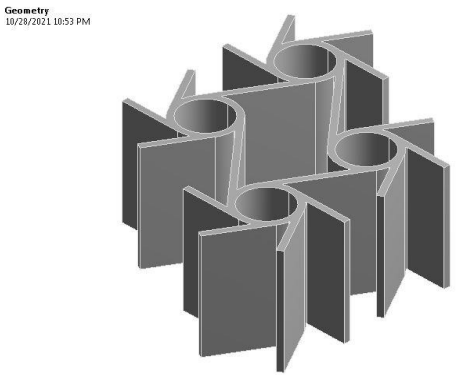


Fig 4.18 Model of Hexa-Chiral

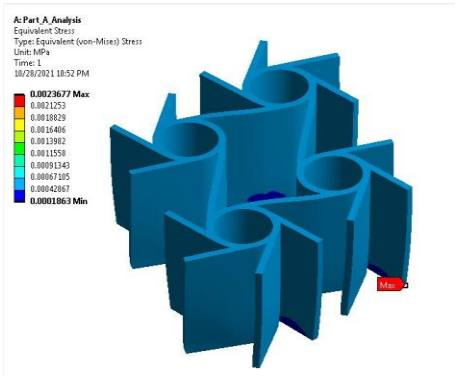


Fig 4.19 Equivalent stress of Hexa-Chiral

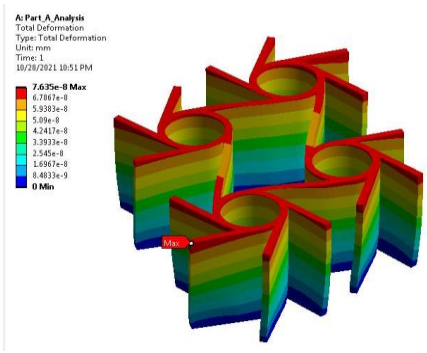


Fig 4.20 Equivalent stress of Hexa-Chiral

- The Hexa- Chiral Honeycomb is one of the chiral shapes used for the analysis and the ligaments or ribs are diagonal to each other and connected to adjacent cylinder loads from 500Pa to 1500Pa are applied with intervals of 250Pa and the stress increases drastically but surprisingly we observed that the percentage of increase decreases drastically compared to 500Pa with 1250Pa from 16.6% to 5%, which shows the Hexa-chiral shape can tolerate loads and can resist buckling since the energy absorption is tremendously better than conventional honeycomb.

Tetra-Chiral Honeycomb

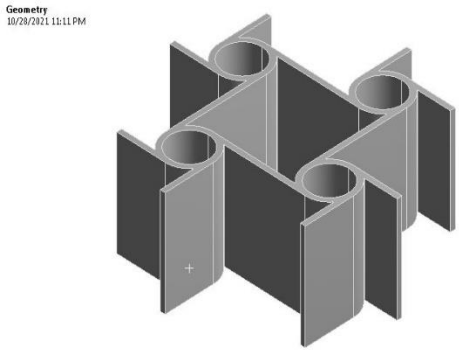


Fig 4.21 Model of Tetra-Chiral

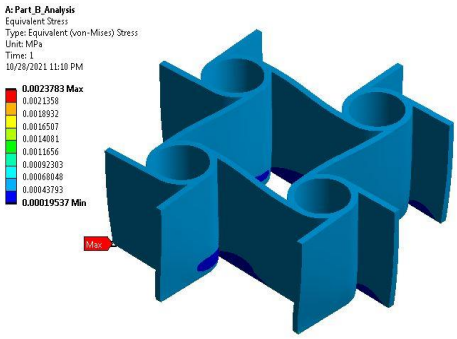


Fig 4.22 Equivalent stress of Tetra-Chiral

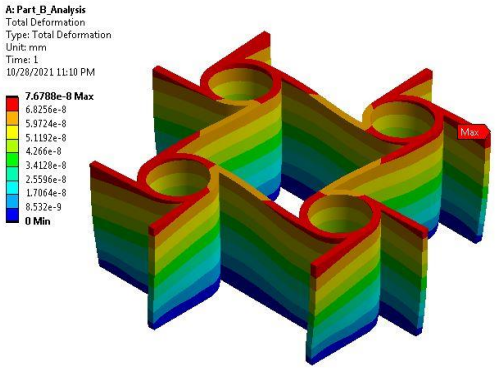


Fig 4.23 Equivalent stress of Tetra-Chiral

- The Anti- Chiral Honeycomb is one of the chiral shapes used for the analysis and the ligaments or ribs are connected tangentially with the help of cylinders loads from 500Pa to 1500Pa are applied with intervals of 250Pa and the stress increases drastically but surprisingly we observed that the percentage of increase decreases drastically compared to 500Pa with 1250Pa from 17% to 5%, which shows the Anti- chiral shape can tolerate loads and can resist buckling since the energy absorption is tremendously better than conventional honeycomb.

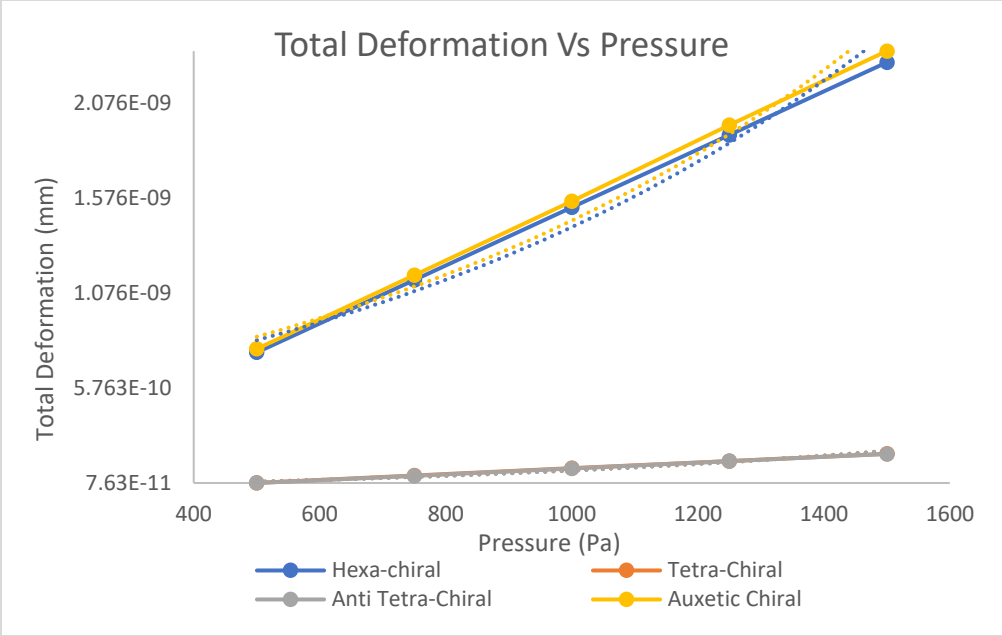


Fig 4.24 Graph plotted between total deformation vs pressure

- The comparison study was conducted for all the four chiral shapes and graph is plotted for the total deformation vs pressure and the results are compared with respect to each other on the behavior of the shapes on different loads and we do observe that Anti-tetra chiral honeycomb has the least deformation and the rest of the three shapes are bit close to each other and the difference is so small.
- Anti-chiral honeycomb has the ribs connected tangentially with the other cylinders and they are perpendicular to each other which provides more strength and resistance to buckling.

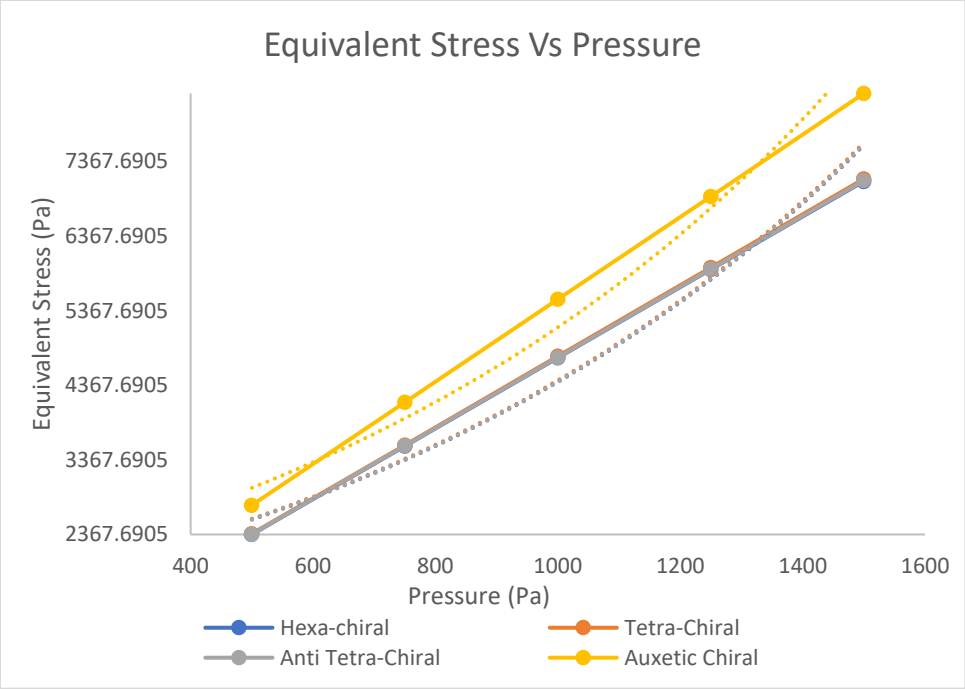


Fig 4.25 Graph plotted between total deformation vs pressure

- The comparison study was conducted for all the four chiral shapes and graph is plotted for the Equivalent stress vs pressure and the results are compared with respect to each other on the behavior of the shapes on different loads and we do observe that Anti-tetra chiral honeycomb has the same resistance as tetra-chiral honeycomb and the results show all the 4 chiral shapes show almost the same strength but the orientation of the ribs has definitely impact on the application based.

Modal Analysis:

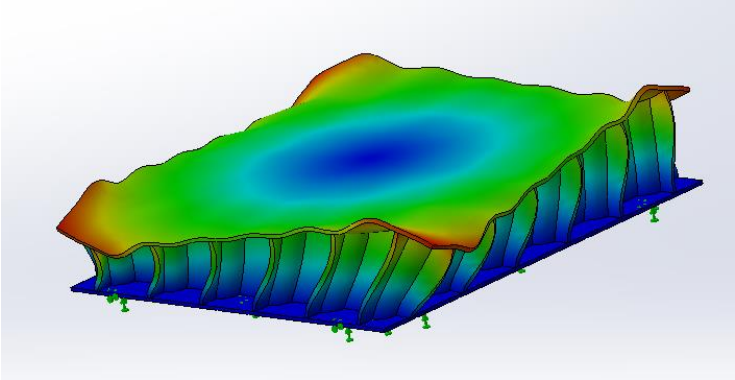

Fig 4.25 First mode of frequency under natural vibration.

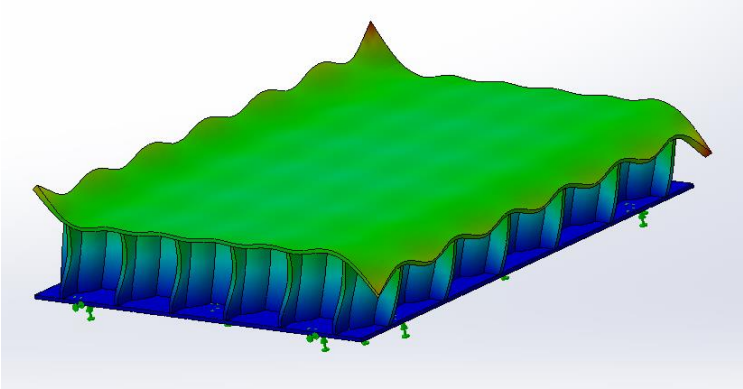

Fig 4.26 Second mode of frequency under natural vibration.

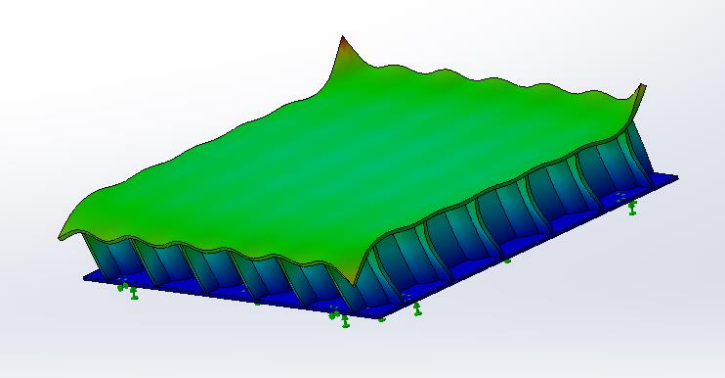

Fig 4.27 Third mode of frequency under natural vibration.

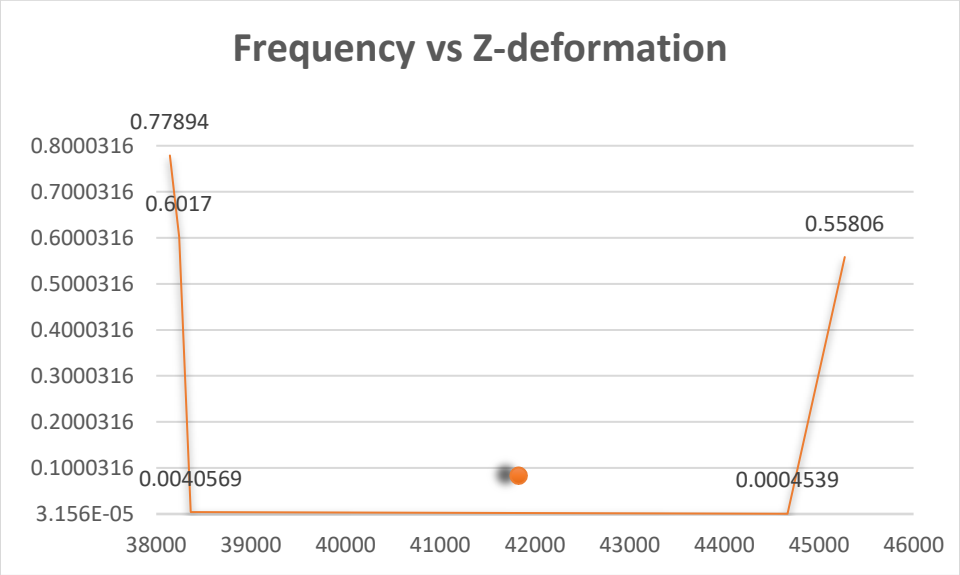


Fig 4.28 Graph plotted between frequency vs Z-direction.

The Modal analysis for the auxetic honeycomb structure has natural frequencies and the nodes and the values are tabulated and the deformation in the z-direction starts decreasing or the first three modes and the there is a constant value for the deformation for the mode 3 and 4. The last two modes have caused the deformation increase in the z-direction.

The Auxetic honeycomb materials have a good stiffness, strength and light weight that is the reason why it is important to study the modes and deformation to know the dynamics and help us understand more on the structures.

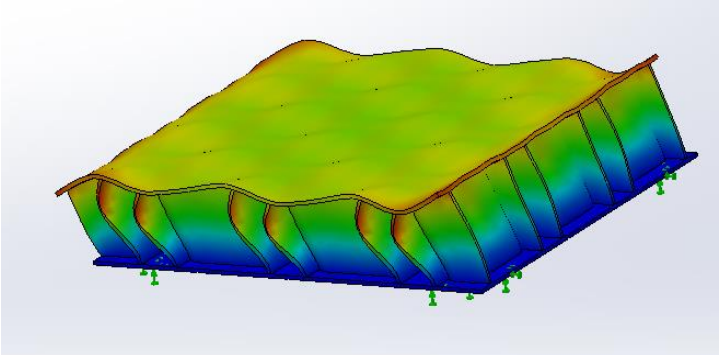

Fig 4.29 First mode of frequency under natural vibration.

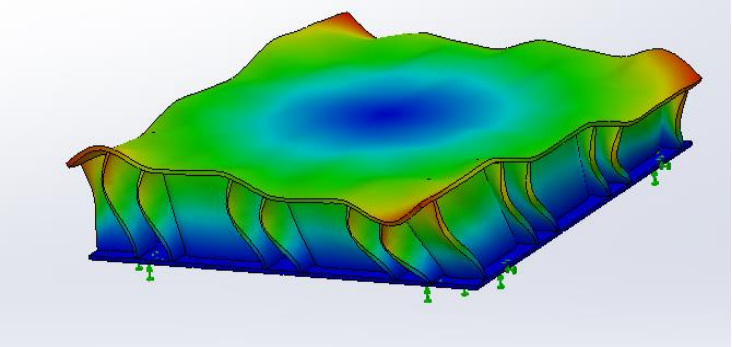

Fig 4.30 Second mode of frequency under natural vibration.

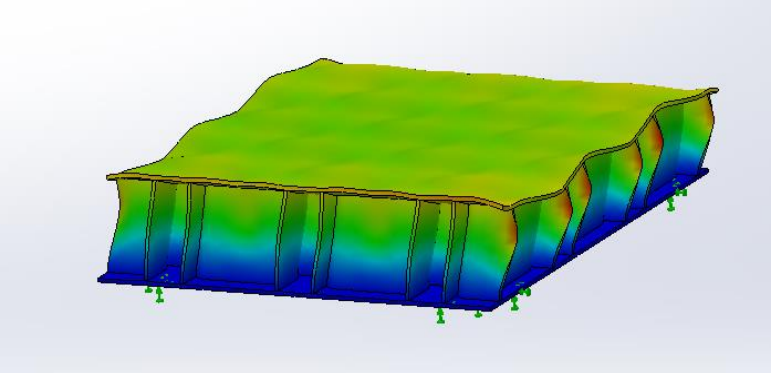

Fig 4.31 Third mode of frequency under natural vibration.

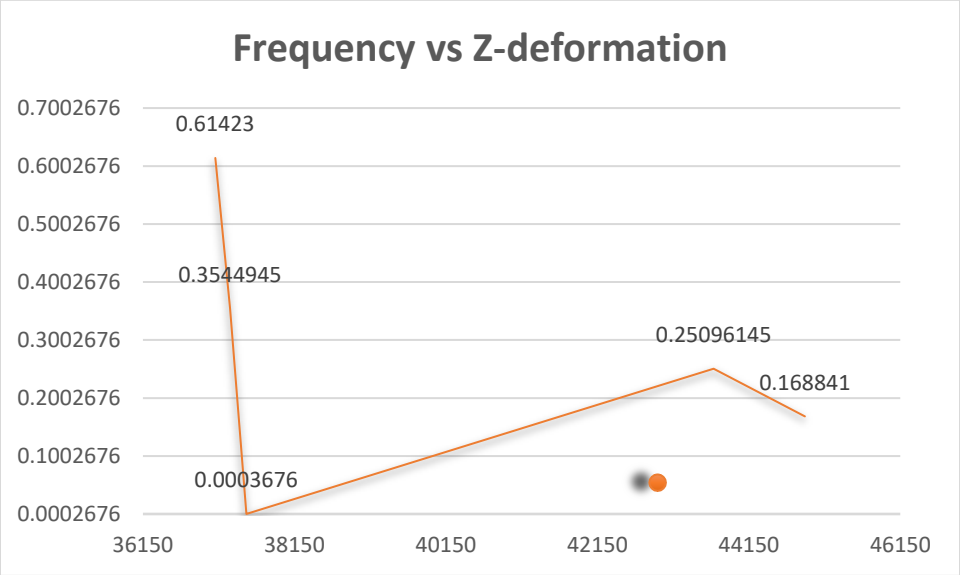


Fig 4.32 Graph plotted between frequency vs Z-direction.

The Modal analysis for the auxetic honeycomb structure has natural frequencies and the nodes and the values are tabulated and the deformation in the z-direction starts decreasing or the first three modes and the there is a substantial increase for the mode 4. The last three modes have caused the deformation decrease in the Z-direction and for the mode 4 &5 the value increases first and then decreases.

The Auxetic honeycomb materials have a good stiffness, strength and light weight that is the reason why it is important to study the modes and deformation to know the dynamics and help us understand more on the structures.

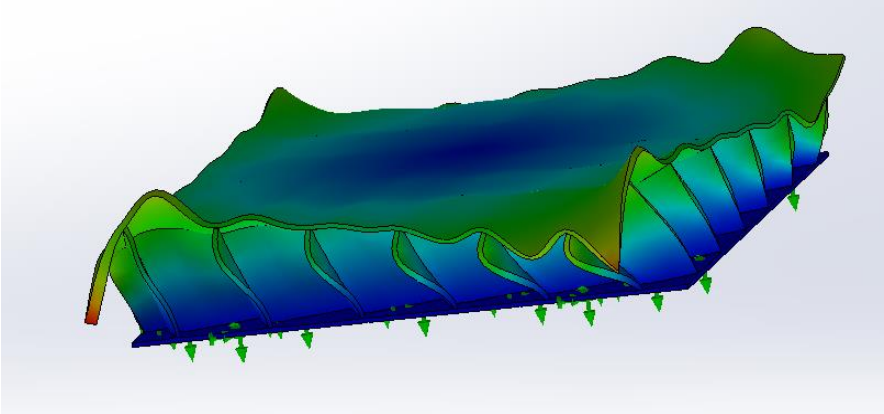

Fig 4.33 First mode of frequency under natural vibration.

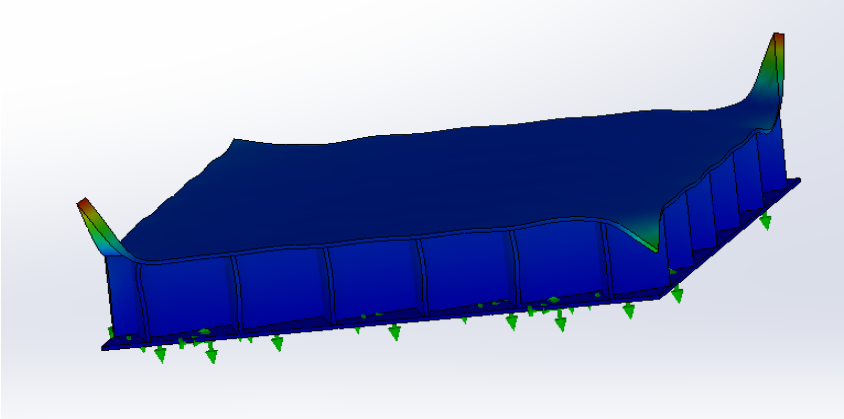

Fig 4.34 Second mode of frequency under natural vibration.

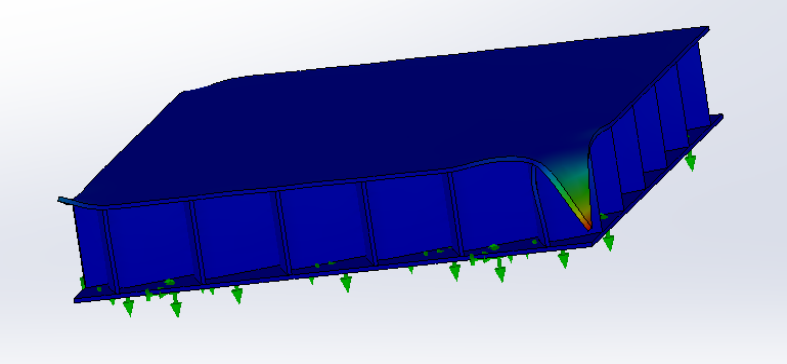

Fig 4.35 Third mode of frequency under natural vibration.

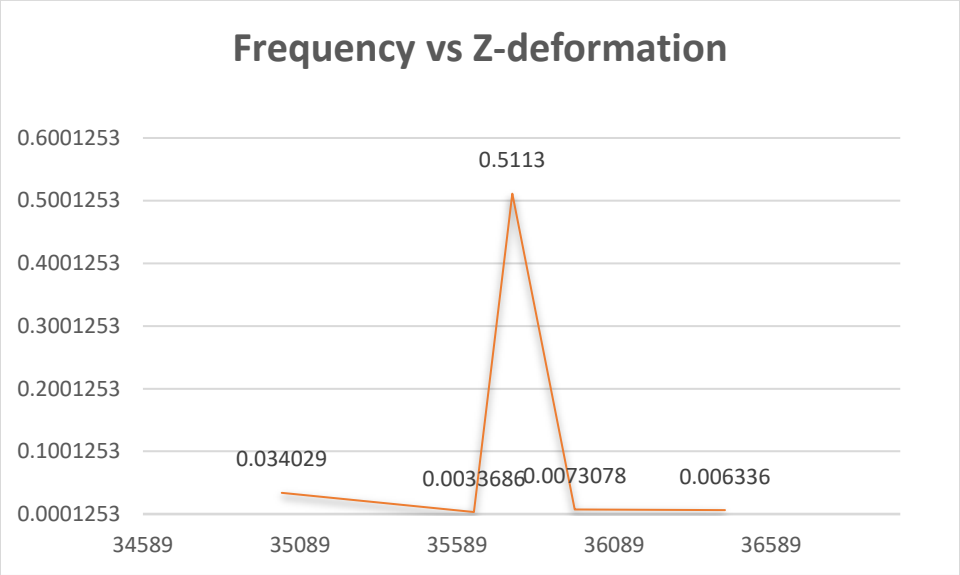


Fig 4.36 Graph plotted between frequency vs Z-direction.

The Modal analysis for the auxetic honeycomb structure has natural frequencies and the nodes and the values are tabulated and the deformation in the z-direction starts decreasing or the first second modes and the there is a sudden peak for the third mode and then increase in the third, fourth and fifth mode.

The Auxetic honeycomb materials have a good stiffness, strength and light weight that is the reason why it is important to study the modes and deformation to know the dynamics and help us understand more on the structures.

Conclusion:

The research presented in this work investigates the various honeycomb structure with varying cell length and comparing the results and simulations are carried out with various loading conditions. Hexagonal has the responsible for isotropic mechanical behavior. The previous findings documented in the literature reported that the chiral lattice is characterizes by elastic properties and large-deformation capabilities, and a negative Poisson's ration of -1 characteristic of auxetic materials.

In plane properties are determined with a refined analysis based on previous studies of the lattice's mechanical behavior, In-plane equivalent elastic constants are determined through existing analytical methods and numerical models with different structural topology. Specially young's modulus and Poisson's ratio indicate that the chiral lattice features in-plane isotropic behavior, confirming previously documented shows the materials has superior high stiffness, high strength. The shear modulus is however the chiral honeycomb structure show very higher than the regular hexagonal honeycomb.

Large deformation are showed in the regular hexagonal honeycomb and the chiral shapes relatively shows lower stresses and deformation for the same amount of loading applied for all the shapes and the boundary conditions, since the chiral honeycomb has sharp edges and there is a high level of stress concentration at the edges with corners. Large deformation capabilities previously suggested in the deign of the truss-core airfoil for both passive and active-morphing applications.

The in-plane direction crushing of honeycomb and investigation of the effects on geometric parameters on the energy absorption provided, simulating the crushing of a single cell honeycomb is sufficient to generate the crushing behavior of honeycomb core with several rows and columns.

With the increase in the angle increases, the deformation of the inclined walls are in the rigid form and the rotational around the plastic hinge and the decrease in the cell angle can cause the stress factor increase and the structure tend to failure, increase in the vertical cell thickness does not change the buckling behavior and the vertical wall thickness are reduced beyond a critical level, the failure mode changes from wrinkling.

Core cell angle did not show any significant effect on the energy absorption. The varying stress reduction with varying cell length had more deformation on the vertical walls compared to the cells with smaller cell length, decreasing the vertical wall length increases the energy absorption. In fact, the total energy absorption for the cells with longer walls are greater compared to the ones with shorter vertical walls since the deformation of vertical walls is relatively higher.

Increasing inclined wall thickness increases the specific energy absorption, the observation for the cell without faces-sheets. Increasing vertical wall thickness increases the SEA and increases the surface deformation.

## Bibliography


1. Statistical finite element analysis of the buckling behavior of honeycomb structures – D Asprone, F Auricchio, C menna, S Moraganti.

2. Cellular Materials in nature and medicine by Gibson and Ashby

3. Honeycomb cores with enhances buckling strength – W. Miller, C.W Smith, K.E Evans

4. Out of plane Mechanical behavior of a side hierarchical Honeycomb - Y Zhang, T Chen, X Xu, Z Hu.

5. Analysis and optimization of parameters influencing the out-of-plane energy absorption of an aluminum honeycomb - S Xie, H Zhou.

6. Finite element analysis of out of plane compressive properties of thermoplastic honeycomb – X fan, verpoest.

7. Ansys workbench tutorial – Dr kent Lawrence.

8. Flatwise buckling optimization of hexachiral and tetrachiral honeycombs - W. Miller, C.W Smith, K.E Evans F scarpa.

9. Buckling and progressive crushing of laterally loaded honeycomb – A Wilbert, WY Jang, S Kyriakides, JF Flocarri.

10. Impact behavior of honeycomb structures with various cell specifications numerical simulation and experiment M yamashita, M Gotoh.

11. Reid, S. R., Reddy T. Y., Peng, C.; "Dynamic Compression of Cellular Structures and Materials", Structural Crashworthiness and Failure, Edited by Norman Jones, Tomasz Wierzbicki, 1993, Elsevier, England, pp. 295-340.

12. Papka, S. D., Kyriakides, S.; "In-plane Compressive Response and Crushing of Honeycomb", J. Mech. Phys. Solids, Vol.42, No.10, Great Britain, 1994, pp.1499- 1532

13. Kellas, S.; Jackson, K.E.; "Deployable system for crash-load attenuation", AHS International 63rd Annual Forum Proceedings, Vol. 2, 2007, pp. 1203-1220

14. Gibson, L.J., Easterling, K.E., Ashby, M.F., "The Structure and Mechanics of Cork", Proceedings of the Royal Society of London, Series A, Mathematical and Physical Sciences, Vol. 377, No. 1769, June 1981, pp. 99-117.

15. Gibson, L.J., Ashby, M.F., Zhang, J., Triantafillou, T.C.; "Failure Surfaces for Cellular Materials under Multiaxial Loads – I. Modeling", International Journal of Mechanical Science, 1989, Vol. 31, No. 9. pp. 635-663

16. McFarland, R. K.; “The Development of Metal Honeycomb Energy Absorbing Elements”, Technical Report No. 32-639, Jet Propulsion Laboratory, 1964.

17. Wierzbicki, T.; “Crushing analysis of metal honeycombs”, International Journal of Impact Eng, 1983; 1(2), pp.157–174.

18. Hoff, N.J. and Mautner, S.E.; “Bending and Buckling of Sandwich Beams”, Journal of the Aeronautical Sciences, 1948, pp. 707–720.

19. Vinson, J.R.; “The Behavior of Sandwich Structures of Isotropic and Composite Materials”, 1999, Technomic Publishing Company, Inc., US.

20. Gibson, L.J.; “Optimization of stiffness in sandwich beams with rigid foam cores”, Materials Science and Engineering, 67, 1984, pp. 125-135.

21. Raj, S.V., Ghosn, L.J.; “Failure maps for rectangular 17-4PH stainless steel sandwiched foam panels”, Materials Science and Engineering A, Vol 474, 2008, pp. 88-95.

22. Lawrence, K. L. (2020). *ANSYS Tutorial Release 2020* (p. 192 pages). Schroff Development Corporation. https://www.sdcpublications.com/Textbooks/ANSYS-Tutorial-Release-2020/ISBN/978-1-63057-394-2/.

23. Lawrence, K. (2012). ANSYS Workbench Tutorial. In *SDC Publications* (14th ed., p. 176). SDC Publications.

24. Lu, G., Shen, J.,Hou. W., Ruan,D., Ong, L.S.; “Dynamic indentation and penetration of aluminum foams”, International Journal of Mechanical Sciences, Vol. 50, 2008, pp. 932-943.

25. Hu, H., Belouettar, S., Potier-Ferry, M., Makdari, A.; “A novel finite element for global and local buckling analysis of sandwich beams”, Composite Structures, 90, 2009, pp. 270-278.

26. Ley, R., Lin, W., Uy, M.: “Facesheet Wrinkling in Sandwich Structures”, NASA/ CR-1999-208984, January 1999.

27. Yamashita, M., Gotoh, M.; “Impact behavior of honeycomb structures with various cell specifications – numerical simulation and experiment”, International Journal of Impact Engineering, Vol. 32, 2005, pp. 618-630.

28. Vinson, J.R.; “The Behavior of Sandwich Structures of Isotropic and Composite Materials”, 1999, Technomic Publishing Company, Inc., US.

29. “Metal Handbooks”, American Society for Metals, 1985, pp. 6.32-6.35.

30. Reid, S. R., Reddy T. Y., Peng, C.; “Dynamic Compression of Cellular Structures and Materials”, Structural Crashworthiness and Failure, Edited by Norman Jones, Tomasz Wierzbicki, 1993, Elsevier, England, pp. 295-340

31. Brentjes, J.; “Honeycomb as an Energy Absorbing Material”, AIAA/ASME 8th Structures, Structural Dynamics and Materials Conference, 1967, pp. 468- 473.

32. Olympio, K. R., Gandhi, F., “Zero-υ cellular honeycomb flexible skins for onedimensional wing morphing”, Collection of Technical Papers - 48th AIAA/ASME/ASCE/AHS/ASC Structures, Structural Dynamics, and Materials Conference, Waikiki, HI, United States, pp. 374-401.

33. Thornton, P.H., Mahmood, H. F., Magee, C. L.; “Energy Absorption by Structural Collapse”, Structural Crashworthiness, Edited by Norman Jones, Tomasz Wierzbicki, 1983, pp. 96-117.

34. Papka, S. D., Kyriakides, S.; “In-plane Compressive Response and Crushing of Honeycomb”, J. Mech. Phys. Solids, Vol.42, No.10, Great Britain, 1994, pp.1499- 1532

35. Thornton, P.H., Mahmood, H. F., Magee, C. L.; “Energy Absorption by Structural Collapse”, Structural Crashworthiness, Edited by Norman Jones, Tomasz Wierzbicki, 1983, pp. 96-117.

36. Gibson, J. L, Ashby, M. F.; Cellular Solids, Cambridge University Press, 2nd edition 1997.

37. Ubels, L.C., Wiggenraad, J.F.M.; “Increasing the Survivability of Helicopter Accidents Over Water”, NLR-TP-2002-110, February 2002, National Aerospace Laboratory, Netherlands

38. Sareen, A.K.; Smith, M.R.; Hashish, E.; “Crash analysis of an energy-absorbing subfloor during ground and water impacts”; Annual Forum Proceedings - American Helicopter Society, Vol. 2, 1999, pp. 1603-1612.

39. Fasanella, E.L.; Jackson, K.E.; Sparks, C.E.; Sareen, A.K.; “Water impact test and simulation of a composite energy absorbing fuselage section”; Journal of the American Helicopter Society, Vol. 50, No. 2, April 2005, pp. 150-164.

40. Wittlin, G.; Smith, M.; Sareen, A.; Richards, M.; “Airframe water impact analysis using a combined MSC/DYTRAN - DRI/KRASH approach”; Annual Forum Proceedings - American Helicopter Society, Vol. 2, 1997, pp. 1138-1150.

41. Tho, C.; Sparks, C.E.; Sareen, A.K.; “Hard surface and water impact simulations of two helicopter subfloor concepts”; 60th AHS Annual Forum, Vol. 2, 2004, pp. 1474-1489.

42. Thomson, R. G, Goetz, R. C.; “NASA/FAA General Aviation Crash Dynamics Program – A Status Report”, Journal of Aircraft, August 1980, Vol. 17, No. 8, pp. 584-590.

43. Anghileri, M.; Castelletti, L.L.; Invernizzi, F.; Mascheroni, M.; “Water impact of a filled tank”; 30th European Rotorcraft Forum, v 2005, 30th European Rotorcraft Forum, 2005, pp. 363-375

44. Bolukbasi, A.O.; “Development of an analysis methodology for crash impacts on soft soil”; Annual Forum Proceedings - American Helicopter Society, Vol. 1, 1998, pp. 297-304.

45. Desjardins, S.; “The evolution of energy absorption systems for crashworthy helicopter seats”, Journal of the American Helicopter Society, Vol. 51, No. 2, April, 2006, pp. 150-163.

46. Barquet, H. ; Sarlin, P.;“Development of a crashworthy composite fuselage and landing gear”, Annual Forum Proceedings - American Helicopter Society, Vol. 2, 1992, pp. 1421-1430

47. Wharton, Jr., C.L.; “High energy absorption landing gear for VTOL aircraft”, Society of Automotive Engineers -- Papers, No. 174C, January 1960, p 22

48. Stephens, B.E., Evans, W. L. III;“Application of skid landing gear dynamic drop analysis”, Annual Forum Proceedings - American Helicopter Society, Vol. 2, 1999, pp. 1644-1652.

49. Jackson, K.E.; Boitnott, R.L.; Fasanella, E.L.; Jones, L.E.; Lyle, K.H.; “A summary of DOD-sponsored research performed at NASA Langley's impact dynamics research facility” Journal of the American Helicopter Society, Vol. 51, No. 1, January, 2006, pp. 59-69

50. Fasanella, E.L. Jackson, K.E.; Lyle, K. H.; “Finite element simulation of a fullscale crash test of a composite helicopter”, Journal of the American Helicopter Society, Vol. 47, No. 3, July, 2002, pp. 156-168.

51. Bolukbasi, A.; “Active crash protection systems for UAVs”; AHS International 63rd Annual Forum, Vol. 2, 2007, pp. 1246-1252.

52. Lyle, K.H.; Jackson, K.E.; Fasanella, E.L.; “Development of an ACAP helicopter finite element impact model”; Journal of the American Helicopter Society, Vol. 45, No. 2, April 2000, pp. 137-142.

53. Kellas, S.; Jackson, K.E.; “Deployable system for crash-load attenuation”, AHS International 63rd Annual Forum Proceedings, Vol. 2, 2007, pp. 1203-1220

54. Abd El-Sayed, F.K., Jones, R., Burgess, I.W.; "A Theoretical Approach to the Deformation of Honeycomb Based Composite Materials", Composites, Vol. 10, No. 4, October 1979, pp. 109-214.

55. Gibson, L.J., Ashby, M.F., Zhang, J., Triantafillou, T.C.; "Failure Surfaces for Cellular Materials under Multiaxial Loads – I. Modeling", International Journal of Mechanical Science, 1989, Vol. 31, No. 9. pp. 635-663.

56. Triantafillou, T.C., Zhang, J., Shercliff, T.L., Gibson, L.J., Ashby, M.F.; "Failure Surfaces for Cellular Materials under Multiaxial Loads – II. Comparison of Models with Experiments", International Journal of Mechanical Science, 1989, Vol. 31, No. 9, pp.665-678.

57. Masters, I. G., Evans, K. E.; "Models for the Elastic Deformation of Honeycombs", Composite Structures, Vol. 35, 1996, pp. 403-422

58. Honig, A.; Stronge, W.J., "In-Plane Dynamic Crushing of Honeycomb. Part II: Application to Impact", International Journal of Mechanical Sciences, Vol. 44, 2002, pp. 1697-1714

59. Goldsmith, W., Sackman, J. L., "An Experimental Study of Energy Absorption in Impact on Sandwich Plates", Int. J. Impact Eng., Vol. 12, No. 2, 1992, pp. 241- 262

60. McFarland, R. K.; "The Development of Metal Honeycomb Energy Absorbing Elements", Technical Report No. 32-639, Jet Propulsion Laboratory, 1964

61. Plantema, F.J.; "Sandwich Construction: The Bending and Buckling of Sandwich Beams, Plates, and Shells", 1966, John Wiley & Sons, Inc., US.

62. Cote, F., Deshpande, V. S., Fleck, N. A., Evans, A. G.; " The Out-of-plane Compressive Behavior of Metallic Honeycombs", Materials Science and Engineering, A 380, 2004, pp. 272-280.

63. Rao, K. M., 1985, "Buckling Analysis of Anisotropic Sandwich Plates Faced with Fiber Reinforced Plastics," AIAA J., 23(8), pp. 1247-1253.

64. Aiello, M. A., and Ombres, L., 1997, "Local Buckling Loads of Sandwich Panels made with Laminated Faces," Composite Structures, 38(1-4), pp. 191-201.

65. Birman, V., and Bert, C. W., 2004, "Wrinkling of Composite-Facing Sandwich Panels Under Biaxial Loading," Journal of Sandwich Structures and Materials, 6, pp. 217-237.

66. Gdoutos, E. E., Daniel, I. M., and Wang, K. A., 2013, "Compression Facing Wrinkling of Composite Sandwich Structures," Mechanics of Materials, 35, pp. 511–522.

67. Campanile, L. and Sachau, D., “Belt-rib concept: a structronic approach to variable camber,” Journal of Intelligent Material Systems and Structures, vol. 11, no. 3, pp. 215 – 224, 2000.

68. Dempsey, B. M., Eisele, S., and McDowell, D. L., “Heat sink applications of extruded metal honeycombs,” International journal of heat and mass transfer, vol. 48, pp. 527 – 535, 2005.

69. Diaz, A., Haddow, A., and Ma, L., “Design of band-gap grid structures,” Structural Multidisciplinary Optimization, vol. 29, no. 6, pp. 418–431, 2005.

70. Dos Santos E Lucato, S., McMeeking, R., and Evans, A., “Actuator placement optimization in a kagome based high authority shape morphing structure,” Smart Materials and Structures, vol. 14, no. 4, pp. 869 – 875, 2005.

71. Doyle, J., “A spectrally-formulated finite element for longitudinal wave propagation,” Int. Journal of Analytical and Experimental Modal Analysis, vol. 3, pp. 1–5, 1998.

72. Eringen, A. C., “Linear theory of micropolar elasticity,” Journal of Mathematics and Mechanics, vol. 15, no. 6, pp. 909–923, 1966.

73. Evans, A. G., Hutchinson, J. W., Fleck, N. A., Ashby, M. F., and Wadley, H. N., “The topological design of multifunctional cellular materials,” Progress in Material Science, vol. 46, pp. 309 – 327, 2001.

74. Gonella, S. and Ruzzene, M., “Homogenization and equivalent in-plane properties of two-dimensional periodic lattices,” International Journal of Solids and Structures, 2008.

75. Grediac, M., “Finite element study of the transverse shear in honeycomb cores,” International Journal of Solids and Structures, vol. 30, no. 13, pp. 1777 – 1788, 1993.

76. Herbert, E. G., Oliver, W. C., and Pharr, G. M., “On the measurement of yield strength by indentation,” Philosophical Magazine, vol. 86, no. 33, pp. 5521–5539, 2006.

77. Hoff, N., “Thermal barrier – structures,” American Society of Mechanical Engineers – Papers, pp. 6 –, 1954.

78. Hussein, M. I., Hamza, K., Hulbert, G., and Saitou, K., “Optimal synthesis of 2d phononic crystals for broadband frequency isolation,” Waves in Random and Complex Media, vol. 17, no. 4, pp. 491–510, 2007.

79. Kelvin, L., Baltimore Lectures on Molecular Dynamics and the Wave Theory of Light. C. J. Clay and Sons, London, U.K., 1904.

80. Lakes, R. S. and Benedict, R., “Noncentrosymmetry in micropolar elasticity,” Internal Journal of Engineering Science, vol. 20, no. 10, pp. 1161 – 1167, 1982.

81. March, J., Advanced Organic Chemistry: Reactions, Mechanisms, Structure. John Wiley and Sons, New York, NY, fourth ed., 1992.

82. Masters, I. G. and Evans, K. E., "Models for the elastic deformation of honeycombs," Composite Structures, vol. 35, no. 4, pp. 403–422, 1996.

83. McGowan, A. M. R., Cox, D. E., Lazos, B. S., Waszak, M. R., Raney, D. L., Siochi, E. J., and Paul Pao, S., "Biologically-inspired technologies in NASA's morphing project," Proceedings of SPIE - The International Society for Optical Engineering, vol. 5051, pp. 1 – 13, 2003.

84. Mohammadi, B., "Fluid dynamics computation with NSC2KE," Tech. Rep. 0164, INRIA, 1994. [69] Monner, H. P., Sachau, D., and Breitbach, E., "Design aspects of the elastic trailing edge for an adaptive wing," October 1999.

85. Moored, K. W. and Bart-Smith, H., "The analysis of tensegrity structures for the design of a morphing wing," Journal of Applied Mechanics, Transactions ASME, vol. 74, no. 4, pp. 668 – 676, 2007.

86. Nowak, A. M., Chiral nuclear dynamics. Singapore, River Edge, NJ, 1996.

87. Psarobas, I. E., "Phononic crystals, sonic band-gap materials," Special Issue of the Journal of Structural, Physical, and Chemical Aspects of Crystalline Materials, vol. 220, no. 9-10, 2005.

88. Roache, P. J., Verification and Validation in Computational Science and Engineering. Hermosa Publishers, Albuquerque, New Mexico, 1998.

89. Ruzzene, M., Scarpa, F., and Soranna, F., "Wave beaming effects in twodimensional cellular structures," Smart Materials and Structures, vol. 12, no. 3, pp. 363 – 372, 2003.

90. Sigmund, O. and Jensen, J., "Systematic design of phononic band-gap materials and structures by topology optimization," Phylosophical Transactions of the Royal Society London, Series A (Mathematical, Physical and Engineering Sciences, vol. 361, no. 1806, pp. 1001–1019, 2003.

91. Spadoni, A. and Ruzzene, M., "Structural and acoustic behavior of chiral trusscore beams," Procedings of the ASME IMECE 2004 Noise Control and Acoustic Division, Anaheim, CA, November 2004.

92. Tibert, A. and Pellegrino, S., "Review of form-finding methods for tensegrity structures," International Journal of Space Structures, vol. 18, no. 4, pp. 209 – 223, 2003.

93. Wang, A. J., Kumar, R. S., and McDowell, D. L., “Mechanical behavior of extruded prismatic cellular metals,” Mechanics of advanced materials and structures, vol. 12, pp. 185 – 200, 2005.

94. Wlezien, R., Horner, G., McGowan, A., Padula, S., Scott, M., Silcox, R., and Simpson, J., “The aircraft morphing program,” Proceedings of SPIE - The International Society for Optical Engineering, vol. 3326, pp. 176 – 187, 1998.

95. Agarwal, B. D. and Broutman, L. J., Analysis and Performance of Fiber Composites. John Wiley, New York, 1980.

96. Bathe, K.-J., Finite Element Procedures. Upper Saddle River, NJ: Prentice Hall, 1st ed., 1996.

97. Bornengo, D., Scarpa, F., and Remillant, C., “Morphing airfoil concept with chiral core structure,” I MECH E Part G, Journal of Aerospace Engineering, vol. G3, no. 8, pp. 185–192, 2005.

98. Buter, A., Ehlert, U. C., Sachau, D., and Breitbach, E., “Adaptive rotor blade concepts, direct twist and camber variation,” 2000.

99. Caddock, B. D., Evans, K. E., and Masters, I. G., “Honeycomb cores with negative Poisson ratio for use in composite sandwich panels,” Proceeding of the ICCM/VIII, vol. 3-E, 1991.